BOLETÍN GEOLÓGICO Y MINERO
2022, VOL. 133 (2), 135-161
ISSN: 0366-0176
http://dx.doi.org/10.21701/bolgeomin/133.2/006

Boletín Geológico y Minero

RESEARCH ARTICLE

The elemental sulfur ore deposit of Salmerón: Las Minas de Hellín basin (Late Miocene, SE Spain)

El depósito de azufre elemental de Salmerón: cuenca de Las Minas de Hellín (Mioceno Superior, SE España)

Javier García-Veigas[1], Domingo Gimeno[2], Victoriano Pineda[2], Dionisio I. Cendón[3], Mónica Sánchez-Román[4], David Artiaga[1], Gemma Bembibre[2]

[1] CCiTUB, Centres Científic i Tecnològics, Universitat de Barcelona, 08028 Barcelona, Spain, garcia_veigas@ub.edu, dartiaga@ub.edu
[2] Departament de Mineralogia, Petrologia i Geologia Aplicada, Universitat de Barcelona, 08028 Barcelona, Spain. domingo.gimeno@ub.edu, vpinedagon@ub.edu, g.bembibre@outlook.es
[3] ANSTO, Australian Nuclear Science and Technology Organization, Kirrawee DC, NSW 2322, Australia, dce@ansto.gov.au
[4] Earth Science Department, Vrije Universiteit Amsterdam, 1081HV Amsterdam, the Netherlands, m.sanchezroman@vu.nl

Corresponding author: garcia_veigas@ub.edu (Javier García-Veigas)

Key points

Two different elemental sulfur bodies (USB and LSB) have been recognized in Las Minas de Hellín basin (Spain)

Native sulfur extensively exploited in underground mines in Las Minas correspond to the LSB hosted in gypsum beds of an evaporitic unit

Native sulfur in the USB, hosted in a carbonate-diatomite unit, is considered as bioepigenetic

ABSTRACT

Strata-bound elemental sulfur deposits occur in different circum-Mediterranean Miocene sedimentary successions containing evaporites and high amounts of organic matter. It is widely known that bacterial sulfate reduction processes are the triggering mechanisms involved in the origin of hydrogen sulfide and the subsequent native sulfur. However, in most of these sedimentary successions, there is controversy over whether elemental sulfur formed in the basin floor, as the same time as the sediments (biosyngenetic), or later, during diagenesis (bioepigenetic). Las Minas de Hellín basin, in the SE Spain, contains one of the largest elemental sulfur deposits in Europe. Based on data recovered from mining company (1903 -1960) and a borehole campaign performed by MINERSA between 1987 and 1988, two native sulfur ore bodies are recognized. The upper sulfur body is hosted by carbonates and diatom-rich levels, whereas the lower sulfur body, only exploited in underground mines now closed, is hosted by gypsum. This work shows a petrological and geochemical study of core samples from the upper sulfur body in the Salmerón area (Murcia), 500 m west of the widely exploited area of Las Minas de Hellín (Albacete). In Salmerón, elemental sulfur occurs as pseudomorphs after primary sedimentary gypsum as well as filling fractures and bed joints. The elemental sulfur replacement is also related to calcification and silicification of the sedimentary biomediated dolomite. The mineralization is considered bioepigenetic formed during early diagenesis. Contribution from hydrothermal waters circulating through adjacent faults are not ruled out.

Keywords: Betic Range; Early diagenesis; Elemental sulfur; Evaporites; Miocene.

Article History:
Received: 17/01/2022
Accepted: 03/03/2022

Puntos clave

Hemos diferenciado dos niveles de azufre elemental (USB y LSB) en la cuenca de Las Minas de Hellín (España)

La mineralización de azufre nativo intensamente explotada en galerías es del nivel inferior (LSB) formado en una unidad evaporítica

La mineralización de azufre del nivel superior (USB), desarrollada en una unidad carbonatado-diatomítica, la consideramos como bioepigenética

RESUMEN

Depósitos de azufre elemental de tipo estratoligado, asociados a evaporitas y niveles ricos en materia orgánica, se encuentran en diferentes series del Mioceno de la cuenca Mediterránea. Existe un consenso general en aceptar que el ácido sulfhídrico, y el posterior azufre elemental, se originaron por mecanismos de sulfato reducción bacteriana. Sin embargo, todavía hay discusión sobre su origen en los sedimentos del fondo de las cuencas (depósitos biosingenéticos), o durante la diagénesis (depósitos bioepigenéticos). La cuenca de las Minas de Hellín contiene uno de los mayores depósitos de azufre elemental explotados de Europa. Dos diferentes niveles mineralizados se han identificado a partir de datos recuperados de la antigua compañía minera (1903–1960) y de una campaña de sondeos realizados por MINERSA en los años 1987 y 1988. El nivel superior aparece en un tramo de carbonatos y diatomitas, mientras que el inferior, solo explotado en minería subterránea, lo hace en yesos. Este trabajo presenta un estudio petrológico y geoquímico de muestras de sondeos del nivel de azufre nativo superior en Salmerón (Murcia), 500 m al W de la extensa explotación en subsuelo, ahora abandonada, de Las Minas de Hellín (Albacete). El azufre elemental pseudomorfiza yeso primario, rellena fracturas y diastemas, y está acompañado de procesos de calcificación y silicificación del encajante dolomítico. La mineralización se considera bioepigenética formada durante la diagénesis temprana. La participación de fluidos hidrotermales ligados a fracturas no es descartable.

Palabras clave: Azufre nativo; Cordillera Bética; Diagénesis temprana; Evaporitas; Mioceno.

Historial del artículo:
Recibido: 17/01/2022
Aceptado: 03/03/2022

1. Introduction

The Late Miocene lacustrine succession of Las Minas de Hellín basin (southern Spain) contains a strata-bound elemental sulfur deposit that has been exploited since the 15th century until the final closure of underground mining operations in 1960.

Miocene sedimentary successions in the circum-Mediterranean region containing strata-bound elemental sulfur deposits are recognized in Spain (Rouchy *et al*., 1998; Ortí *et al*., 2010), Sicily (Dessau *et al*., 1962; Ziegenbalg *et al*., 2010), Poland (Ivanov, 1968; Pawlowski *et al*., 1979; Parafiniuk, 1989; Gasiewicz, 2000), Egypt (Phillip *et al*., 1994), Turkey (Tekin, 2006) and Iraq (Jassin *et al*., 1999). Elemental sulfur deposits in these sequences are related to the coexistence of: (1) evaporites, (2) organic-rich diatomite deposits, and (3) diagenetic carbonate minerals.

Worldwide strata-bound elemental sulfur deposits related to evaporites and diagenetic carbonates are considered biogenic as result of bacterial sulfate reduction processes in anaerobic conditions (Davis and Kirkland, 1970; Barker *et al*., 1979; Böttcher and Parafiniuk, 1998; Peckmann *et al*., 1999, Labrado *et al*., 2019). Bacterial sulfate reduction (BSR) promotes the transformation of dissolved sulfate to hydrogen sulfide, and other reduced sulfur species, as well as the generation of CO_2 through anaerobic organic matter oxidation. Hydrogen sulfide can be subsequently oxidized to native sulfur in oxygenated waters and the alkalinity increase can cause the precipitation of carbonate minerals (Pierre and Rouchy, 1988, Anadón *et al*., 1992; Vasconcelos and McKenzie, 1997; Machel, 2001; van Lith *et al*., 2002).

Sulfuretums (Baas-Becking, 1925) represent microbial communities of sulfate-reducing and sulfide-oxidizing bacteria (SRB and SOB) which are the most productive elemental sulfur producing microorganisms in sedimentary environments (e.g. anaerobic subaqueous environments like sea and lake floors and sediment pore-waters). Elemental sulfur (S^0) is produced by anoxygenic sulfur bacteria. Then, it can be then oxidized to sulfate (SO_4^{2-}) by sulfur-oxidizing bacteria or transformed to hydrogen sulfide (H_2S), by sulfur-reducing bacteria.

In some anaerobic sedimentary environments, H_2S produced by SRB can combine with sedimentary reactive iron (Fe^{2+}) to form iron sulfides (Fe_2S), being pyrite the most common resulting mineral. In the absence of Fe^{2+}, and other oxidizing metals, the abiotic partial oxidation of H_2S to S^0 only occurs in a very narrow range of Eh-pH conditions (Brookins, 1988). In such abiotic conditions, most of the H_2S generated is completely oxidized to SO_4^2. Formation and preservation of elemental sulfur deposits is unlikely because S^0 consists of a dynamic intermediate term in the oxidation process of H_2S.

Biogenic elemental sulfur deposits can be biosyngenetic (sedimentary) or bioepigenetic (early/late diagenesis) in origin (Ruckmick *et al*., 1979; Davis and Kirkland, 1979). Biosyngenetic sulfur occur in euxinic, organic-rich, restricted marine or lacustrine environments. Davis and Kirkland (1979) offer, as an example, the coastal lagoons in the shores of the Bay of Bengal which are half of the year inundated by seawater during the monsoon season. Marine dissolved sulfate is microbially reduced to hydrogen sulfide in the organic-rich soils and then oxidized to sulfur when the seawater recedes. Preservation of biosyngenetic sulfur occurrences in the sedimentary record of coastal settings is unlikely because of the redox changes characteristic of such environments.

Trace concentrations of S^0 have been analytically reported in many marine and non-marine recent sediments (Kaplan *et al*., 1963; Nrigu,1968; Jørgensen, 1977; Troelsen and Jørgensen, 1981; Francois 1986; Passier *et al*., 1999; Wijsman *et al*., 2001). In these settings, elemental sulfur is limited to biologically active sulfuretums. Preservation of elemental sulfur in layers or nodules have never been reported in modern (Holocene) sediments. The youngest nodules of elemental sulfur have been recognized in the Pleistocene-Holocene transition in the lake Petén Itzá (Guatemala) and interpreted as diagenetic in origin (Hodell *et al*., 2006).

Bioepigenetic sulfur deposits can form in sedimentary rocks and uncemented sediments by combination of sulfate (mineral and/or dissolved), large amounts of organic matter (trapped in sediments and/or hydrocarbon-rich fluids), and anaerobic conditions promoting the development of sulfate-reducing bacteria. Bioepigenetic sulfur deposits can be classified as cap rock sulfur deposits and strata-bound sulfur deposits (Ruckmick *et al*., 1979; Davis and Kirkland, 1979). While cap rock sulfur deposits are always related to late diagenetic processes, strata-bound sulfur deposits can be formed during early and late diagenesis.

Unfortunately, the definition of 'early diagenesis' is a controversial topic in sedimentology. Di-

agenesis occurs at any time subsequent to the deposition, or mineral precipitation, in the sediment-water interface. Berner (1980) defines 'early diagenesis' as the changes occurring during burial to a few hundred meters in which sediments are continually filled with water. Lithification, the process by which sediments are converted in solid sedimentary rocks occurs during early diagenesis.

Cumulated evaporites precipitated in the basin water and deposited in the basin floor are considered as sediments. Evaporites and carbonates precipitated in the basin floor (sediment-water interface) should be considered as authigenic minerals but also as sediments, they are not diagenetic. Nevertheless, evaporites, carbonates and other minerals formed interstitially in sediments must be considered as authigenic as well as early diagenetic minerals.

There is still controversy interpreting the Late Miocene strata-bound sulfur deposits in Poland (Carpathian foredeep) and Sicily (Central Sicilian basin) as biosyngenetic (Dessau *et al.*, 1962; Ivanov, 1968; Gasiewicz, 2000) or as bioepigenetic (Pawlowski *et al.*, 1979; Parafiniuk, 1989; Ziegenbalg *et al.*, 2010). The distinction between biosyngenetic or bioepigenetic strata-bound elemental sulfur deposits is difficult and requires of a precise petrographic control of the relationships between elemental sulfur occurrences and their host-rock.

Native sulfur occurrences in Las Minas de Hellín basin, and in the nearby Cenajo basin (Figure 1), can be observed in different abandoned open-pits and in waste piles of underground old mines widely exploited during the centuries XIX and XX. These limited occurrences were originally interpreted as bioepigenetic (Elízaga, 1994; Calvo and Elízaga, 1994) and subsequently as biosyngenetic (Servant-Vildary *et al.*, 1990; Gimeno, 1994; Lindtke *et al.*, 2011; Ortí *et al.*, 2014b; Pozo *et al.*, 2016).

Despite of large volume of waste mounds resulted from the ancient underground mining operations, waste samples are very scarce in elemental sulfur because of subsequent weathering. Information of the buried sulfur ore beds in Las Minas de Hellín is limited to their number, depths

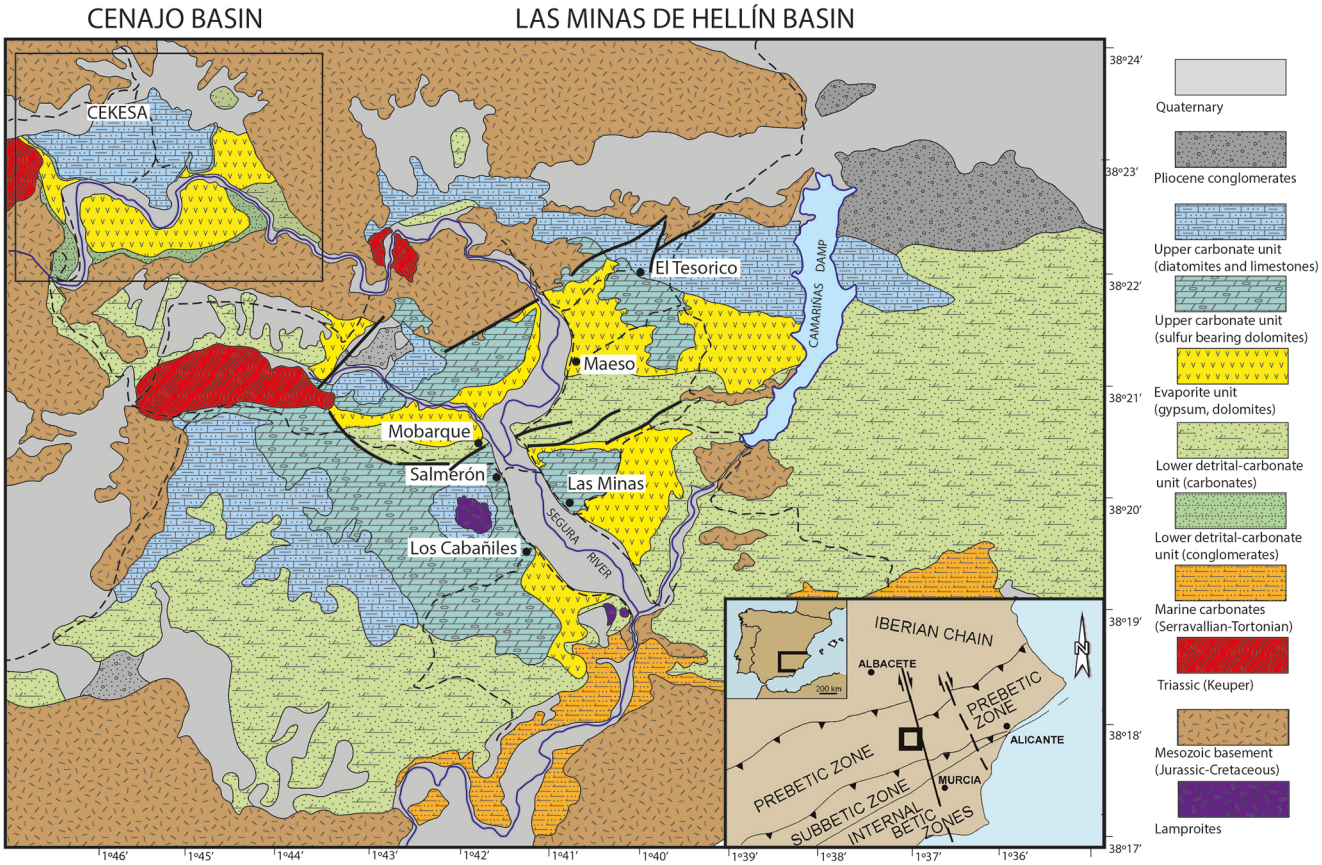

Figure 1. Geological map of Las Minas de Hellín and the Cenajo basins (Murcia and Albacete, Spain). Map adapted from unpublished MINERSA (1988) 1:10000 map. Lithostratigraphic units correspond to those defined by Calvo *et al.* (2000).

Figura 1. Mapa geológico de las cuencas de Las Minas de Hellín y del Cenajo (Murcia y Albacete). Adaptado del mapa 1:10000, no publicado, de MINERSA (1988). Las unidades litoestratigráficas corresponden a las definidas por Calvo *et al.* (2000).

and sulfur contents (Meseguer, 1924, summarized in Gimeno, 1994).

Between 1987 and 1988, after the definitive closure of underground mining operations in 1960, a borehole prospecting campaign was conducted in Las Minas de Hellín basin by the company MINERSA. A total of 27 boreholes were drilled in the western margin of the Segura river (Figure 2). We have had access to the unpublished original geological maps and core descriptions performed by MINERSA.

Two elemental sulfur bodies can be differentiated in the MINERSA boreholes drilled through the alluvial deposits of the Segura river close to the township of Salmerón (Murcia) and nearby of the abandoned mined area of Las Minas de Hellín (Albacete) (Figure 2).

This work presents a petrographic study of core samples from the upper sulfur body (USB) intersected in Salmerón which is stratigraphically equivalent to the outcropping sulfur body in Las Minas de Hellín abandoned quarries and in old mines in the Mobarque and Cenajo areas (Figure 3). The lower sulfur body (LSB) in the MINERSA boreholes, which correspond to the buried mining works in Las Minas, is out of the scope of this study. The aim of this paper is to propose a genetic model for the USB which spread across the Salmerón, Las Minas, and Mobarque areas of Las Minas de Hellín basin, and in the neighboring Cenajo basin.

2. Geological setting

The Betic Cordillera, southern Spain, is an alpine orogen formed by the collision between the European and African plates. Its evolution, together with the Rif Cordillera in northern Africa, controlled the Mediterranean restriction that caused the onset of the Messinian Salinity Crisis (MSC) and deposition of evaporites. Extensional tectonics during Tortonian and Early Messinian caused the Betic Cordillera to be configured in a set of sedimentary basins separated by ranges. During the uplift of the cordillera, most of these basins

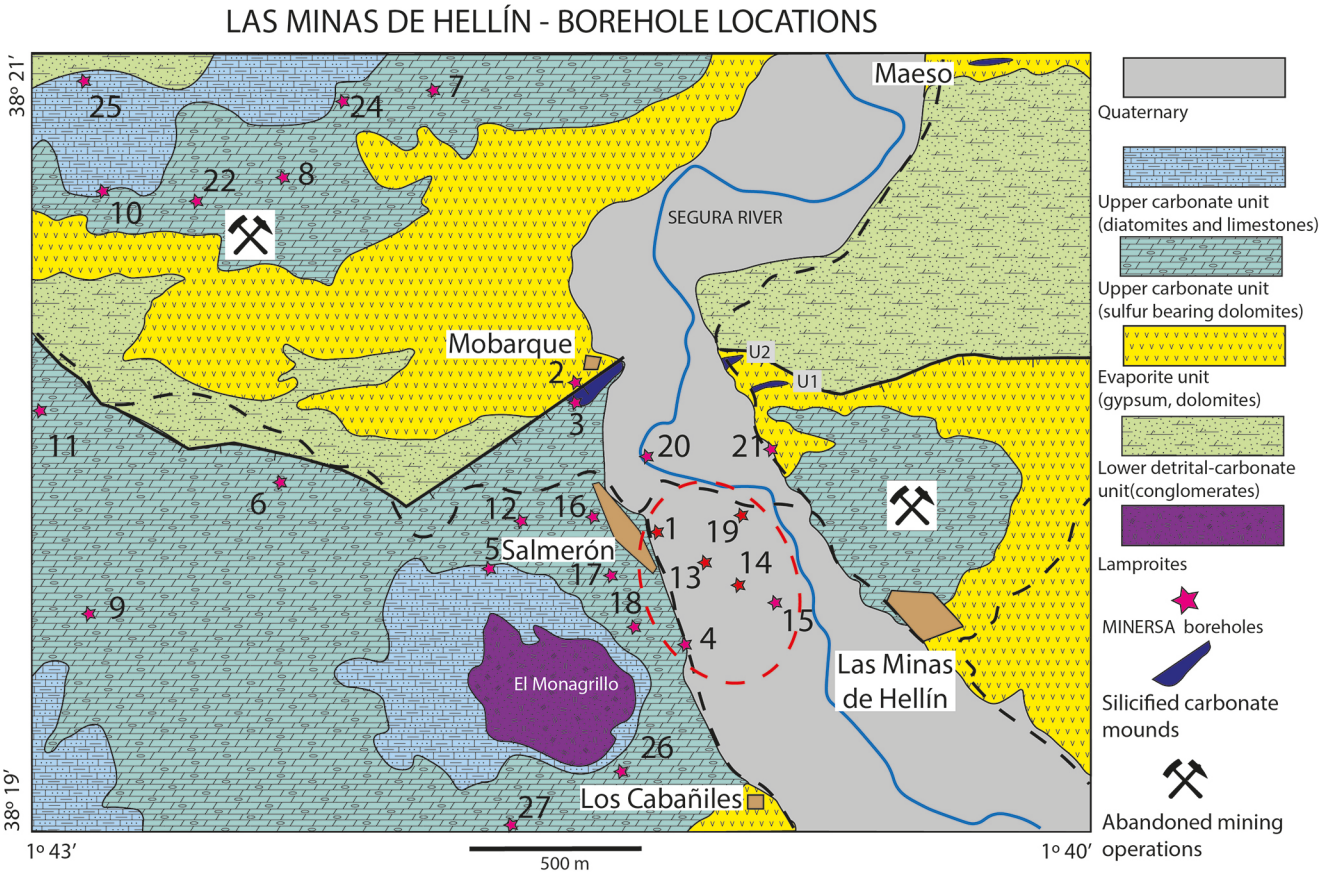

Figure 2. Geological map of the Las Minas de Hellín sulfur ore deposit (adapted from unpublished MINERSA map. Location of boreholes drilled by MINERSA and of carbonate mounds described in Pozo *et al.* (2016).

Figura 2. Mapa geológico del depósito mineralizado superior en Las Minas de Hellín (adaptado del mapa no publicado de MINERSA). Situación de los sondeos de MINERSA y de los montículos carbonatados descritos en Pozo *et al.* (2016).

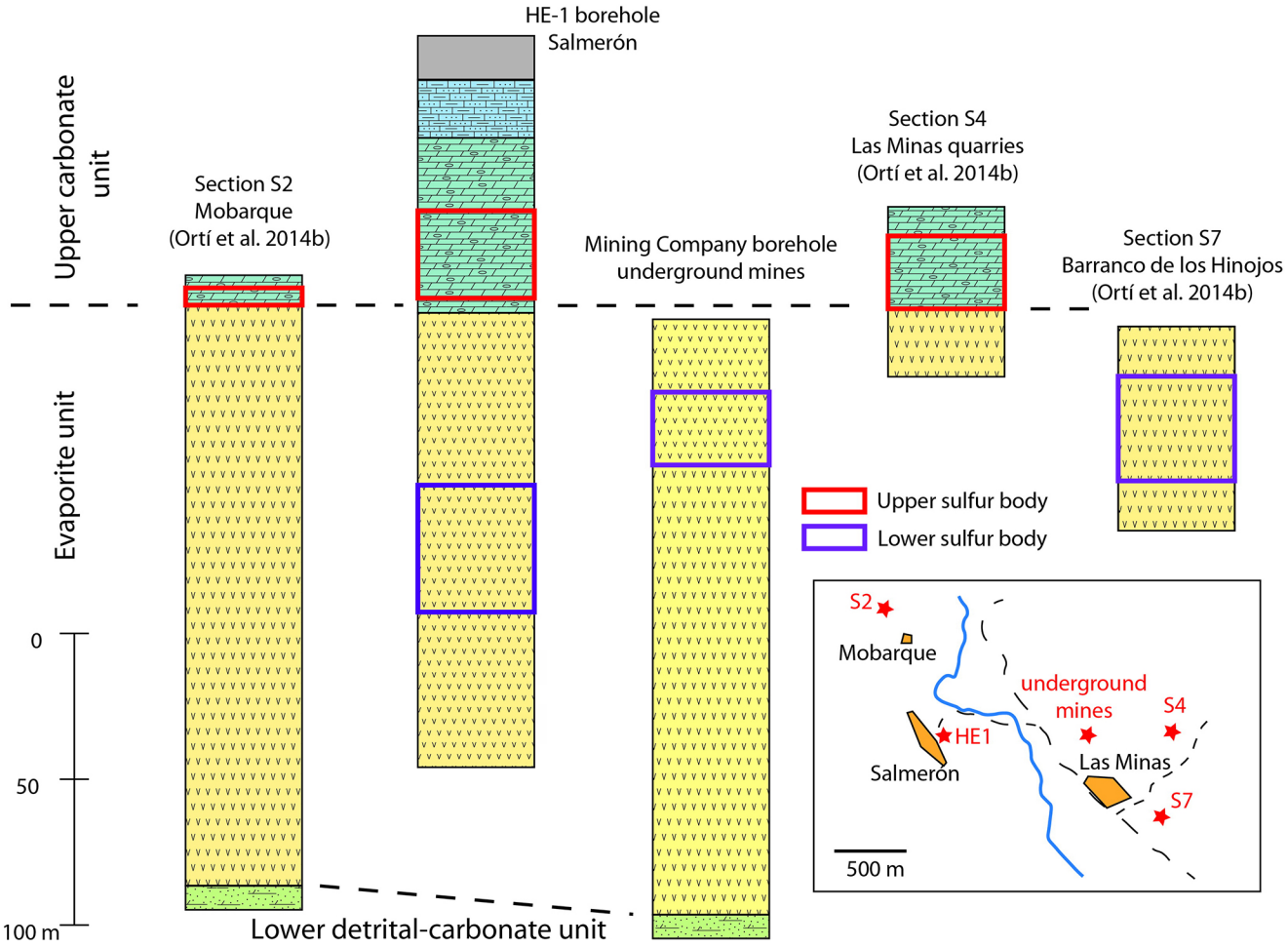

Figure 3. Correlation chart of different boreholes and sections (Ortí *et al.*, 2014b) with location of the two elemental sulfur bodies in Las Minas de Hellín basin.

Figura 3. Diagrama de correlación de diferentes sondeos y secciones (Ortí *et al.*, 2014b) con posición de los dos niveles mineralizados de azufre elemental en la cuenca de Las Minas de Hellín.

evolved from marine to continental conditions (Sanz de Galdeano and Vera, 1991; Playà *et al.*, 2000; Martín *et al.*, 2014). In the Late Messinian, only the most westward basins, nowadays close to the Mediterranean coastline, remained flooded by marine waters recording MSC marine deposits.

Las Minas de Hellín basin, also known as Las Minas-Camarillas basin, is one of the intramountane Neogene Betic basins located in the eastern sector of the Prebetic Zone (External Zones of the Betic Cordillera) in SE Spain, between the cities of Albacete and Murcia (Figure 1). There are several basins in the area, being Las Minas de Hellín the largest (~160m^2). Las Minas de Hellín and the Cenajo basins (Figure 1) are the only ones incorporating evaporites and elemental sulfur deposits. The area is characterized by a transfer fault zone crossed by three main strike-slip dextral faults with NW-SE directions (Martín-Velázquez *et al.*, 1988; Rodríguez-Pascua *et al.*, 2001). Each basin is bounded by W-E normal faults forming graben or half-graben basins. Las Minas de Hellín and the Cenajo basins show an asymmetrical tectonic pattern with higher activity in their northern basin margins (Rodríguez-Pascua *et al.*, 2001, 2003).

The stratigraphy and sedimentology of the Neogene basins in the area, including Las Minas de Hellín and the Cenajo basins, is well-known (Calvo *et al.*,1978; Elízaga and Calvo, 1988; Elízaga, 1994). The Late Miocene coastal lacustrine successions in these basins unconformably overlie Mesozoic terrigenous and carbonate basement units, as well as Middle Miocene marine carbonates (Calvo and Elízaga, 1994; Calvo *et al.*, 2000). The lower part has been assigned to Tortonian by micromammals (Calvo *et al.*, 1978) and the upper part to Messinian from radiometric analyses of pyroclasts and lamproite rocks of the Monagrillo volcano, located in Las Minas de Hellín basin (Bellon *et al.*, 1980; Nobel *et al.*, 1981; Ortí *et al.*, 2014b).

Different lithological and informal stratigraphic units have been proposed by Foucalt *et al*. (1987) and Servant-Vildary *et al*. (1990) respectively. However, none of these authors reported lithostratigraphic descriptions and their terminology have not been subsequently adopted. The simplified summary stratigraphic succession performed by Calvo *et al*. (2000, 2014) is shown in Figure 4. We adopt the informal terminology proposed by Ortí *et al*. (2014b), based on Calvo *et al*. (2004, 2014), in which the Late Miocene sedimentary succession is lithostratigraphically divided, in ascending order, in: (1) lower detrital-carbonate unit, (2) evaporite unit, and (3) upper carbonate unit. Pliocene fluvial gravels unconformably overlay the Late Miocene succession.

The lower detrital-carbonate unit, up to 150m thick, consists of conglomerate turbidites and carbonate beds. Conglomerate clasts derived from resedimentation of Early Tortonian marine carbonate platforms (Calvo and Elízaga, 1994; Elízaga, 1994).

The evaporite unit, up to 200m thick, consists of gypsum and dolomite beds alternating with diatomite-rich and organic-rich (paper-shale) beds. Elemental sulfur occurrences, of little significance, have been recognized in evaporite unit outcrops (Ortí *et al*., 2014b; Pineda *et al*., 2021)

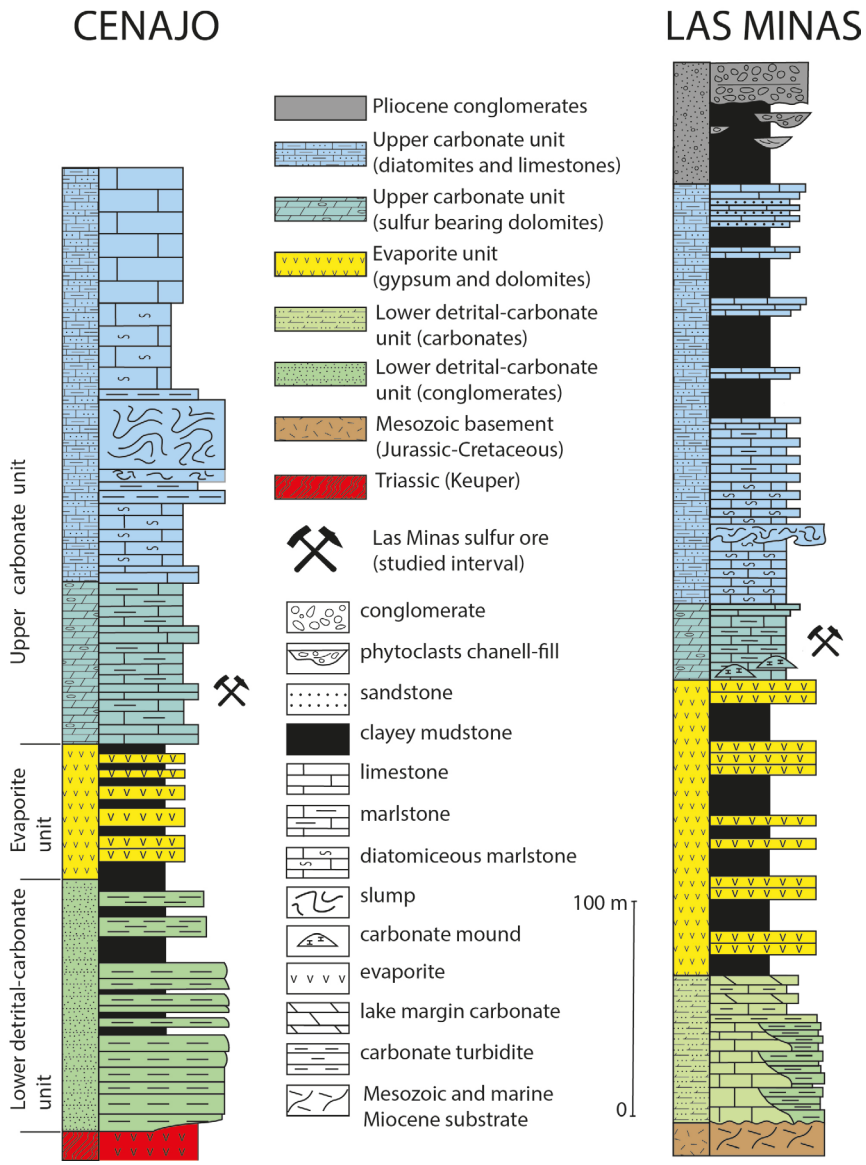

Figure 4. Composite simplified lithostratigraphic sections of Las Minas de Hellín and Cenajo basins (modified from Calvo *et al*., 2014).

Figura 4. Columnas litoestratigráficas simplificadas de las cuencas de Las Minas de Hellín y del Cenajo (modificada de Calvo *et al*., 2014).

The upper carbonate unit consists of a large interval, up to 300m thick, of alternating carbonates and diatomite-rich beds (with marl appearance). Large volumes of elemental sulfur have been exploited at the base of the upper carbonate unit. In this sulfur bearing basal part, local mounds of strongly folded and/or brecciated carbonates, partly silicified, have been interpreted as formed by hydrothermal springs as either the lake floor and within unconsolidated sediment discharges (Pozo *et al*., 2016).

Upwards in the upper carbonate unit, sediments become progressively enriched in diatomaceous beds and locally intercalate slump deposits, some of them of decametric thickness. Elízaga (1994) suggested that these large-scale slump deposits are related to the seismic activity associated with the extrusive, potassium-rich lamproitic volcanism of the Monagrillo hill (Figure 1). The uppermost part is characterized by mixed siliciclastic-carbonate lacustrine deposits (Calvo *et al*., 2000).

Assignation of the currently elemental sulfur occurrences in the abandoned quarries of Las Minas de Hellín to one of these lithostratigraphic units can be misleading. Indeed, the boundary between the top of the 'evaporite unit' and the base of the 'upper carbonate unit' can be easily mistaken because both units consist of alternations of dolomite and diatomite-rich beds/layers. As informal lithostratigraphic units, the only difference between them is the presence or absence of intercalated sedimentary gypsum layers (Ortí *et al*., 2014b; Pineda *et al*., 2021). Probably due to the abundance of diagenetic gypsum (satin spar), the elemental sulfur in Las Minas de Hellín abandoned quarries was incorrectly assigned to the evaporite unit by Servant-Vildary *et al*. (1990) and Lindtke *et al*. (2011). However, these quarries correspond to the base of the 'upper carbonate unit' (Figure 3) because do not contain sedimentary gypsum layers.

Although both the upper carbonate and the evaporite units show a wide distribution in Las Minas de Hellín basin (Figure 1), native sulfur occurrences are limited to three reduced areas. These areas correspond the three mining concessions working between 1890 and 1960: (1) the Mari Paz concession, southwest of Salmerón (~90Ha), (2) the Coto Menor concession in Las Minas de Hellín area (~760Ha), and (3) the Guillermo concession in the Barranco de Mobarque (also referred as Moharque) (~73Ha). These three areas are located close to the Mobarque fault, two in the southern hanging wall, the other in the relatively lifted foot wall (figures 1 and 2).

Based on the distribution of old mining operations (underground mine entrances, firing kilns, mining waste piles and abandoned quarries) we can recognize that the USB, hosted in the base of the upper carbonate unit, was underground exploited in the north of the Mobarque fault (Guillermo concession) and in the Salmerón area (Mari Paz concession), and in open quarries in Las Minas de Hellín (Coto Menor concession) (Figure 3).

The LSB, ~60m below the USB, is located within the evaporite unit and was exclusively underground mined in Las Minas de Hellín area. The underground mining in Las Minas de Hellín was active from 1903 to 1960. It has been estimated that around 270000 tonnes (Gimeno, 1994) of buried elemental sulfur were extracted during this period. Unfortunately, there is no information concerning the lithology of the buried mineralized levels. Macrolenticular gypsum, together with elemental sulfur, can be recognized in many waste piles, showing that gypsum is the host rock in the LSB. According to information retrieved from mining company documents, the equivalent ore levels outcrop southeast of the village, in the Barranco de los Hinojos, in the eastern margin of the road from Las Minas to Agramón (Figure 3). There, discrete elemental sulfur occurrences appear in gypsum beds of the evaporite unit.

3. Material and methods

A total of 27 exploratory boreholes were drilled in Las Minas de Hellín basin by the MINERSA company (Figure 2). Boreholes were drilled in two prospecting areas in which elemental sulfur was previously mined in small galleries and quarries: the Salmerón area (Mari Paz concession), and the Mobarque area (Guillermo concession). These areas are located in the southern and northern blocks of the Mobarque fault respectively (Figure 2). Coordinates and depths of each borehole are listed in Ortí *et al*. (2014b).

Synthetic columns of the MINERSA borehole HE-1 (Salmerón), the sections S2 (Mobarque), S7 (Barranco de los Hinojos) and S4 (Las Minas quarries) of Ortí *et al*. (2014b), and of a borehole log included in an old mine map of the underground galleries in Las Minas de Hellín, are correlated in Figure 3. Note that all previous works interpreting elemental sulfur occurrences in Las

Minas de Hellín basin (Servant-Villardy *et al*., 1990; Lindtke *et al*., 2011) correspond to the USB.

The two sulfur ore bodies are recognized in the Salmerón HE-1 borehole (Figure 3). The USB, 30 m thick (60 - 90m bgs), is placed at the base of the upper carbonate unit, whereas the LSB, 50m thick (150 - 200m bgs), is within a gypsum succession assigned, in this paper, to the evaporite unit but previously assigned to the top of the lower carbonate-detrital unit by Ortí *et al*. (2014b). The Salmerón USB, hosted by carbonates, correlates with the sulfur occurrences in Las Minas de Hellín abandoned quarries, while the LSB, hosted by gypsum, is equivalent to the sulfur ore deposit exploited in the underground mines in Las Minas de Hellín.

The MINERSA core recovery was limited to the Salmerón USB. Free sulfur laws higher than 15% were reported in boreholes 1, 4, 13, 14, 15, and 19 in an area of 5km^2 beneath the Segura river alluvium, between the villages of Las Minas de Hellín (Albacete province) and Salmerón (Murcia province) (Figure 2). Continuous cores for petrographic identifications were recovered from 4 boreholes (1, 13, 14 and 19). The present petrographic study has been performed on 50 core samples from these boreholes. Sample positions (depths) in each borehole are indicated in Figure 5.

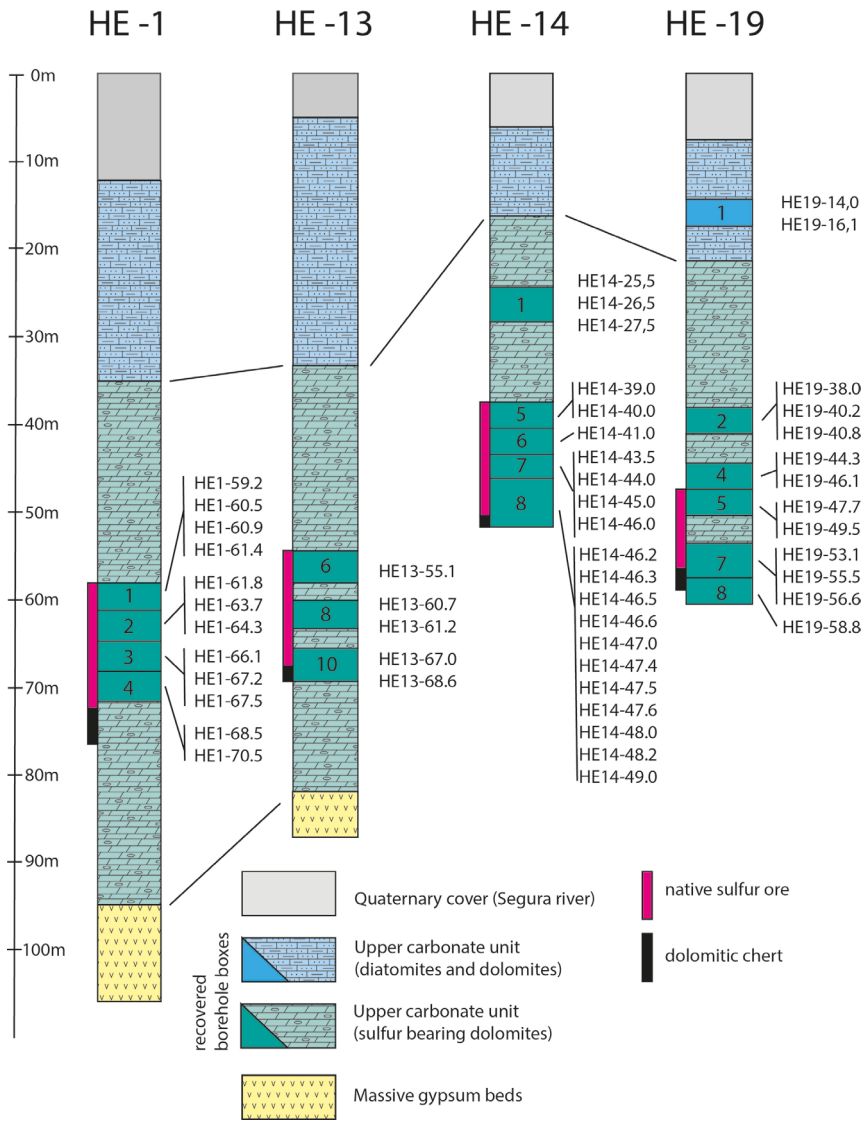

Figure 5. Logs of the MINERSA boreholes in the Salmerón area (Las Minas de Hellín basin). Position of the native sulfur ore deposit (USB) and of the studied samples.

Figura 5. Registros de los sondeos MINERSA en el área de Salmerón (cuenca de Las Minas de Hellín). Posición del nivel mineralizado superior y de las muestras estudiadas.

Core samples have been cut and polished to be directly observed in a large chamber SEM (FEI QUANTA-250) in low vacuum conditions. Small fragments of each sample have been also observed in a high resolution FESEM (JEOL J7100FE). Both microscopes are coupled with SDD EDS detectors (Thermo Fisher UltraDry - Pathfinder Alpine, and Oxford Instruments X-Act – AztecLive, respectively). SEM images have been acquired with Secondary Electron detectors (SE) for topographical information, and with Backscattered Electron detectors (BSE) for chemical (average atomic number) information. Thin sections of 10 selected samples have been observed by optical microscopy. Powdered samples have been analyzed by XRD.

Samples for carbonate isotopic determinations ($\delta^{13}C$ and $\delta^{18}O$) have been grinded with a micro drill device avoiding mixing with other carbonate minerals and components. Isotope analyses have been performed using a Thermo Scientific KIEL III carbonate device at 70ºC, 5 minutes for calcite and aragonites, and 15 minutes for dolomites. The obtained CO_2 was analyzed in a mass spectrometer Thermo Scientific MT 252. Internal standards were calibrated with the international NBS18 and NBS 19 standards reporting analytical precisions of ± 0.10‰ for both $\delta^{13}C$ and $\delta^{18}O$. Isotope compositions are reported relative to Vienna Pee Dee Belemnite (VPDB).

Published isotope data from the evaporite unit (Servant-Vildary *et al.*, 1990; Lindtke *et al.*, 2011; Ortí *et al.*, 2014b; Pineda *et al.*, 2021) and from the upper carbonate unit (Bellanca *et al.*, 1989; Pozo *et al.*, 2016) are incorporated and reviewed in the discussion points.

4. Results

4.1. Mineralogy and petrology

In the studied Salmerón boreholes, the host rock of the USB is mainly dolomite. Four dolomite lithofacies have been distinguished: (1) poor-cemented, 'marly' appearance, dolomites, (2) pseudomorphic massive dolostones (Figure 6A), (3) fine-laminated dolomite beds, often with pseudomorphs (Figure 6B), and (4) broken laminated, breccia dolostones (Figure 6C). In the top of the ore deposit, aragonite layers intercalate with dolomite layers. Both carbonate beds consist of poorly cemented, highly permeable sediments.

The term 'marl', frequently used for shale-like intervals intercalated between dolomites in outcrops of the upper carbonate unit is avoided in this paper because clay minerals are almost absent. The marly, or shale appearance, of these intervals are due to the presence of abundant diatom sheets within dolomite laminae.

Elemental sulfur, in the studied boreholes, occurs as opaque nodules formed by microcrystalline aggregates (figures 6D, 6F, and 7A), and as euhedral translucent crystals filling voids (most of the gypsum casts) (figures 7F and 7G), veins and fractures (figures 6E, 7C and 7D). Most pseudomorphs after gypsum are filled by elemental sulfur (figures 6B, 7B, and 7E) and calcite (Figure 7H). The base of the ore body is partially or completely silicified (figures 6G and 6H), or replaced by calcite.

Microscopically, three dolomite components can be distinguished: (1) equant dolomicrite, (2) prismatic dolomicrite, and (3) prismatic dolospar. Equant dolomicrite consists of rhombohedral crystals, less than 2μm long, often with empty cores and exhibiting dendritic growth patterns (Figures 8A, 8B and 8C). In thin sections, equant dolomicrite forms peletoidal grains. Prismatic dolomicrite crystals are up to 10μm long and frequently coexist with equant dolomicrite (Figures 8D and 8E). Prismatic dolospar crystals, up to 50μm long, show combined scalenohedral and rhombohedral habits (Figures 8F, 8G and 8H). Equant and prismatic dolomicrite crystals are the main components in all dolomite beds. Prismatic dolospar is restricted to the walls (rims) of pseudomorphs and empty casts.

Aragonite layers (Figure 7A) are uncemented and consists of prismatic crystals (Figure 9A). Calcite layers, less than 1mm thick (Figure 9B), consist of anhedral sparite crystals cementing diatomite-rich layers (Figure 9C). Coarse euhedral calcite crystals are filling veins and fractures (figures 9D and 9E). Calcite is often associated with native sulfur. Calcite consists of sparry crystals filling partially (figures 7B, 7E, 10B, 10F and 10H), or wholly (Figure 7H), voids and gypsum casts.

An important primary component of the host rock was gypsum. Primary gypsum crystals were completely dissolved, after lithification, forming empty casts (figures 7F and 7G) and elemental sulfur pseudomorphs after gypsum (figures 7B and 7E), calcite (figures 7B, 7E and 7H), or diagenetic gypsum.

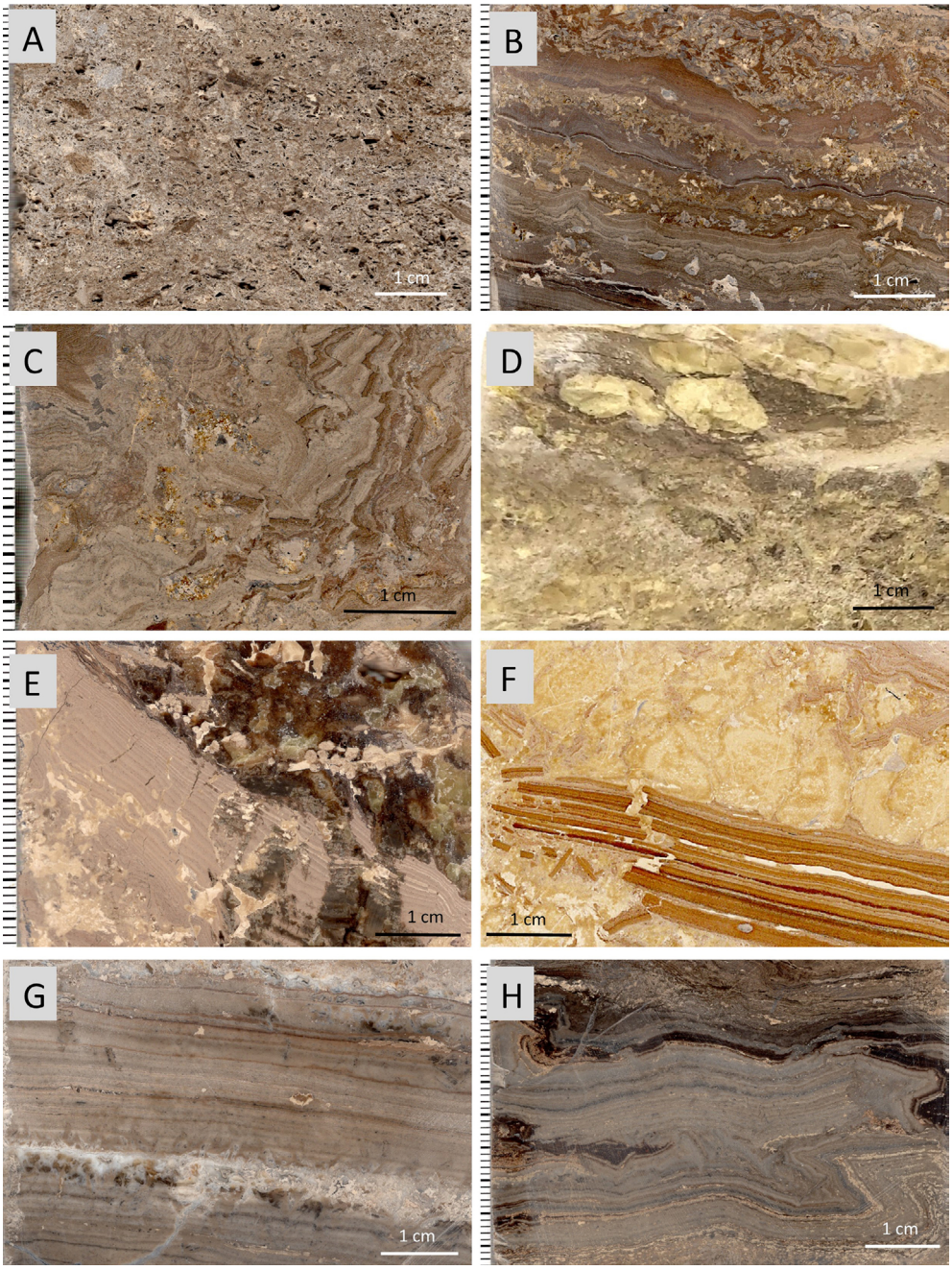

Figure 6. Sulfur-bearing lithofacies (hand samples) of the Salmerón USB (Las Minas de Hellín basin). A) Massive dolomite (dolomicrite) with empty gypsum casts (HE14-47.0 m). B) Laminated dolomite (dolomicrite) with native sulfur pseudomorps after gypsum (HE14-46.2 m). C) Truncated laminated dolomite (dolomicrite) with native sulfur and opal filling voids (HE14-46.5 m). D) Sulfur nodules in a diatomite-rich interval between dolomicrite and aragonite layers (HE1-61.8 m). E) Truncated laminated dolomite (dolomicrite) with native sulfur and calcite filing fractures. Calcite also replace dolomite layers (HE1-63.7 m). F) Fine-laminated dolomite (dolomicrite) truncated by the displacive growth of native sulfur (HE19-49.5 m). G) Partly silicified fine-laminated dolomite (chert). Vertically oriented native sulfur pseudomorphs after gypsum (HE14-48.2 m). H) Partly silicified fine-laminated dolomite (chert) (HE14-46.6 m).

Figura 6. Litofacies de azufre elemental (testigos de sondeo) del nivel mineralizado superior de Salmerón (cuenca de Las Minas de Hellín). A) Dolomitas masivas (dolomicrita) con cavidades huecas de yeso lenticular (HE14-47,0 m). B) Dolomitas laminadas (dolomicrita) con pseudomorfos de yeso reemplazados por azufre (HE14-46,2 m). C) Dolomitas laminadas rotas (dolomicrita) con ópalo y azufre elemental rellenando cavidades (HE14-46,5 m). D) Nódulos de azufre en un intervalo diatomítico entre láminas de dolomita y aragonito (HE1-61,8 m). E) Dolomitas laminadas rotas (dolomicrita) con calcita y azufre elemental rellenando fracturas. La calcita también reemplaza a las láminas de dolomita (HE1-63, 7 m). F) Dolomitas finamente laminadas (dolomicrita) rotas por el crecimiento desplazante de azufre elemental (HE19-49,5 m). G) Dolomita finamente laminada parcialmente silicificada. Pseudomorfos de cristales de yeso de orientación vertical reemplazados por sílice (HE14-48,2 m). H) Dolomita finamente laminada parcialmente silicificada (HE14-46,6 m).

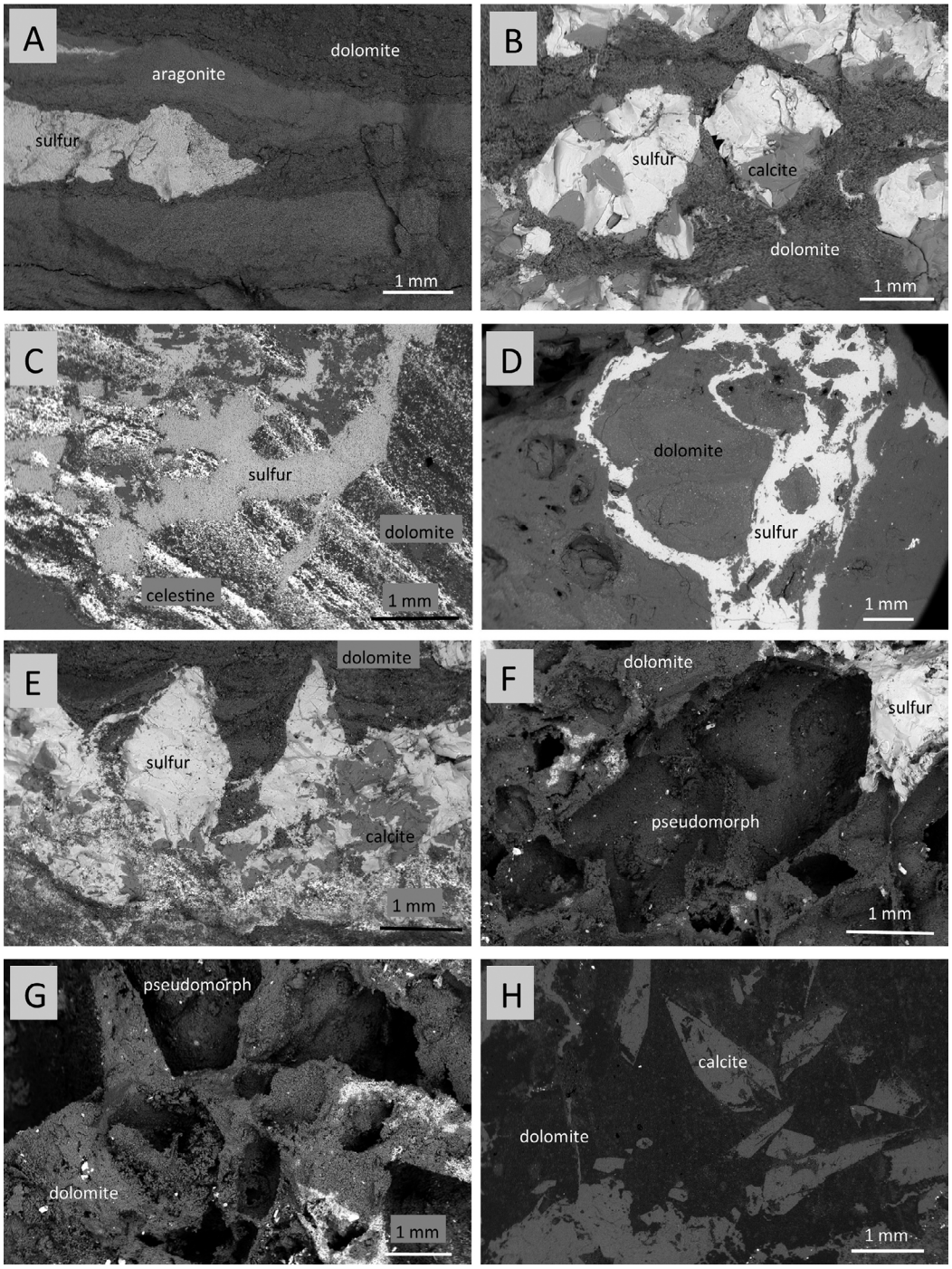

Figure 7. SEM-BSE images of sulfur occurrences in the Salmerón USB (Las Minas de Hellín basin). A) Native sulfur nodules growing in a diatomite-rich layer between dolomicrite and aragonite layers (HE1-61.8 m). B) Native sulfur and calcite pseudomorphs after gypsum (HE1-67.2 m). C) Native sulfur filling veins crosscutting dolomite and celestine layers (HE1-63.7 m). D) Native sulfur filling veins in a massive pseudomorphic dolomite bed (HE14-53.1 m). E) Native sulfur and calcite filling vertically oriented pseudomorphs after gypsum (HE1-67.5 m). F) Empty cast of a twined gypsum crystals (HE14-53.1 m). G) Empty casts of lenticular gypsum crystals partly filled by native sulfur (HE14-53.1 m). H) Calcite pseudomorphs after gypsum (HE1-66.1 m).

Figura 7. Imágenes SEM-BSE de azufre elemental en el nivel mineralizado superior de Salmerón (cuenca de Las Minas de Hellín). A) Nódulos de azufre creciendo en una lámina diatomítica entre láminas de aragonito (HE1-61,8 m). B) Azufre elemental y calcita pseudomorfizando cristales de yeso (HE1-67,2 m). C) Venas de azufre elemental cortando láminas de dolomita y celestina (HE1-63,7 m). D) venas de azufre elemental en una dolomita con cavidades de yeso (HE14-53,1 m). E) Azufre elemental y calcita pseudomorfizando cristales verticalmente orientados de yeso (HE1-67,5 m). F) Moldes de cristales de yeso parcialmente rellenados por azufre elemental (HE14-53,1 m). H) Pseudormorfos de yeso reemplazados por calcita (HE1-66.1 m).

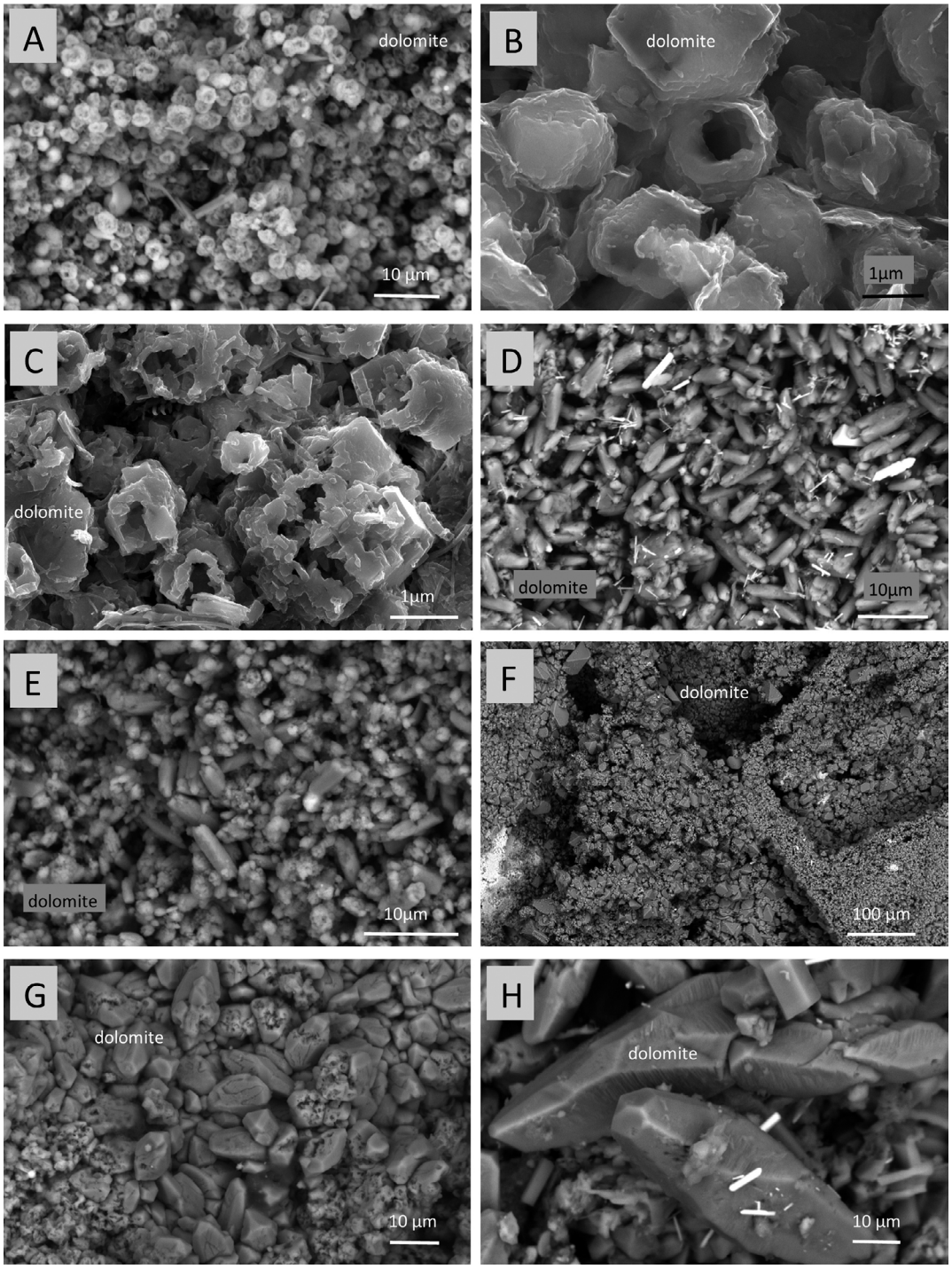

Figure 8. Dolomite components in the host rock of the Salmerón USB (Las Minas de Hellín). A) Equant dolomicrite with empty cores (sample HE1-60.5 m; SEM-BSE). B) Equant dolomicrite (sample HE14-27,5 m; FESEM-SE). C) Dendritic dolomicrite (HE14-25,5 m; FESEM-SE). D) Prismatic dolomicrite and acicular celestine crystals (sample HE1-67.2 m, SEM-BSE). E) Prismatic dolomicrite (sample HE14-41.0 m; SEM-BSE). F) Prismatic dolospar lining empty gypsum casts (sample HE14-47.0 m; SEM-BSE). G) Prismatic dolospar with dolomicrite cores (sample HE19-47.7 m; SEM-BSE). H) Scalenohedral dolospar (sample HE19-55.5 m; SEM-BSE).

Figura 8. Componentes dolomíticos en la roca huésped del nivel mineralizado superior de Salmerón (cuenca de Las Minas de Hellín). A) Cristales equigranulares de dolomicrita con núcleos huecos (HE1-60,5 m; SEM-BSE). B) Cristales equigranulares de dolomicrita (HE14-27,5 m; FESEM-SE). C) Cristales dendríticos de dolomicrita (HE14-25,5 m; FESEM-SE). D) Cristales prismáticos de dolomicrita y aciculares de celestina (HE1-67,2 m, SEM-BSE). E) Cristales de dolomicrita prismática (HE14-41,0 m; SEM-BSE). F) Doloesparita prismática tapizando moldes de cristales de yeso (HE14-47,0 m; SEM-BSE). G) Doloesparita prismática con núcleos de dolomicrita (HE19-47,7 m; SEM-BSE). H) Doloesparita escalenoédrica (HE19-55, 5m; SEM-BSE).

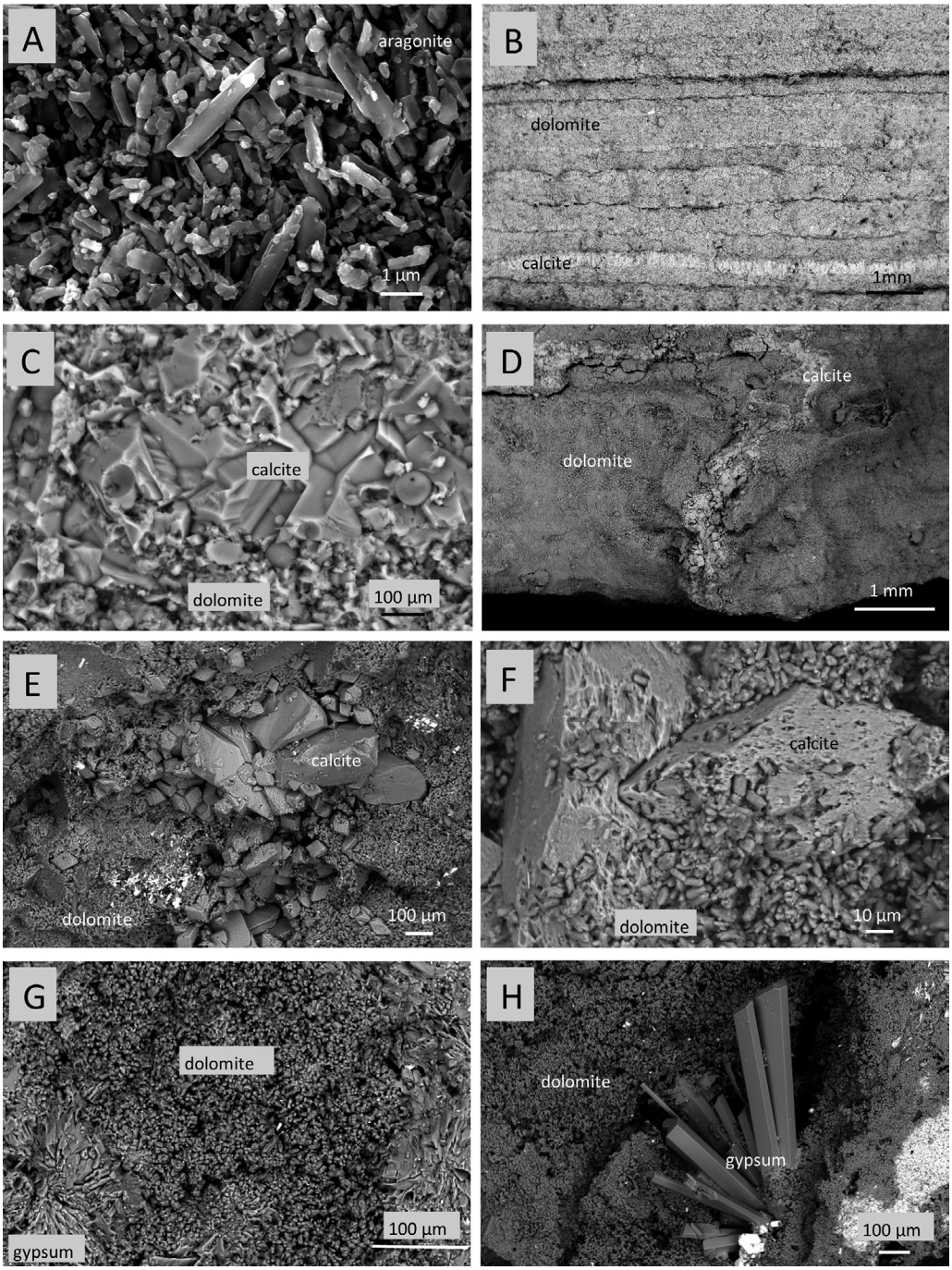

Figure 9. Calcium carbonate and gypsum components in the host rock of the Salmerón USB (Las Minas de Hellín basin). A) Prismatic aragonite crystals (HE19-38.0 m, FESEM-SE). B) Calcite between dolomite layers. Calcite spar crystals cementing originally porous diatomite-rich layers (HE13-61.4 m; SEM-BSE). C) Calcite spar crystals cementing dolomicrite (HE19-40.8 m; SEM-BSE). D) Calcite spar filling a vein crosscutting dolomite layers (HE14-26.5 m; SEM-BSE). E) Calcite spar crystals filling a vein in a dolomicrite layer (HE1-68.5 m; SEM-BSE). F) Calcite crystal cementing dolomicrite in a pokilitic texture (HE1-68.5 m; SEM-BSE). G) Acicular radiating aggregates (efflorescences) cementing porous dolomicrite layers (HE13-60.7 m; SEM-BSE). H) Diagenetic gypsum crystals in a radiating texture (geode) growing into an original (sedimentary) gypsum cast (HE14-53.1 m; SEM-BSE).

Figura 9. Aragonito, yeso y calcita en la roca huésped del tramo mineralizado superior de Salmerón (cuenca de Las Minas de Hellín). A) Cristales prismáticos de aragonito (HE19-38,0 m; SEM-BSE). B) Calcita cementando láminas diatomíticas, altamente porosas, entre láminas de dolomita (HE13-61.4 m; SEM-BSE). C) Calcita esparítica cementando dolomicrita (HE19-40,8 m; SEM-BSE). D) Calcita esparítica en venas cortando láminas de dolomita (HE1-26.5 m; SEM-BSE). F) Cristales de calcita cementando poiquilíticamente dolomicrita (HE1-68,5 m; SEM-BSE). G) Agregados radiales (eflorescencias) de yeso acicular cementando laminas porosas de dolomicrita (HE13-60,7 m; SEM-BSE). H) Cristales de yeso diagenético, tipo geoda, rellenando un molde hueco de yeso (HE14-53.1 m; SEM-BSE).

Although gypsum is recognized by XRD in almost all samples, this mineral phase is entirely diagenetic. Diagenetic gypsum appears as disseminated meshes of acicular crystals (efflorescences) growing into poorly cemented, highly porous, dolomicrite beds (Figure 9G). Radial aggregates of prismatic gypsum crystals, also diagenetic, can be found into empty casts (Figure 9H).

Diatom remains, in a very wide sense, are another important host rock component. High amounts of diatoms and sponge spicules appear disseminated in massive dolostones or forming sheets intercalated between dolomite layers. Margalef (1955) recognizes the abundance of marine and non-marine diatom remains (division *Chrisophyta*, clase *Bacillariophyceae*), and of cysts and flagella of golden-brown algae (division *Chrisophyta*, clases *Chrysophyceae* and *Synurophyceae*). Similar assignations have been later reported by Servant-Vildary *et al*. (1990) and, recently, by Pineda *et al*. (2021).

Organic matter remains, with high sulfur contents, are very abundant in most core samples. Silica phytoliths of undetermined plants (figures 11A and 11B) have been recognized in some samples. High oil generation potential has been determined in the MINERSA boreholes by Permanyer *et al*. (2016).

Celestine is a minor but ubiquitous mineral in the host rock. Celestine crystals are idiomorphic, acicular to prismatic, less than 10μm long (Figure 11C). Some carbonate layers can contain up to 50% of celestine. Celestine appears as disseminated crystals in dolomite beds following sedimentary layering (Figure 7C) and outlining pseudomorphs after gypsum now replaced by calcite and/or chalcedony (Figure 11D).

Authigenic silica components (opal and chalcedony) are abundant, mainly in the base of the sulfur ore body where the host rock can be completely silicified and/or replaced by sparry calcite. Micrometer opal lepispheres coat the surface of the dolospar crystals in empty gypsum casts (figures 10A, 10C, 11E and 11F). Chalcedony eventually fills the casts originally coated by dolospar, opal and/or calcite (figures 10C, 11G,11H).

One of the most relevant lithological features of the sulfur ore host rock is the low content of mud (clay) and detrital components. Scattered sharp edged, silicate grains, probably tuff grains, have been found in different samples. Pyrite framboids are very scarce and when they appear are always oxidized.

4.2. Carbonate isotopes

Samples of different mineralogy (aragonite, dolomite and calcite) have been selected for carbonate isotope determinations. $\delta^{13}C$ and $\delta^{18}O$ data, borehole depths, mineral compositions, and crystal habits of each sample are listed in Table 1.

Borehole	Depth (m)	Mineralogy (type of crystalls)	$\delta^{13}C$	$\delta^{18}O$
HE1	59.2	dolomite (equant dolomicrite)	- 7.58	+ 6.71
	60.5	dolomite (equant dolomicrite)	- 7.99	+ 9.92
	61.8	aragonite	+ 2.63	+ 5.85
	66.1	calcite (sparite)	- 5.64	- 7.22
HE14	26.5	dolomite (equant dolomicrite)	- 4.54	+ 7.19
	41.0	dolomite (prismatic dolomicrite)	- 5.76	+ 9.36
	43.5	dolomite (prismatic dolomicrite)	- 6.29	+ 3.34
	47.0	dolomite (prismatic dolospar)	- 7.12	+ 2.77
	47.6	calcite (sparite)	- 4.40	- 8.06
	48.0	calcite (sparite)	- 4.61	-8.34
HE19	38.0	aragonite	+ 3.71	+ 6.06
	49.5	dolomite (prismatic dolomicrite)	- 5.15	+ 5.34
	53.1	dolomite (prismatic dolospar)	- 8.35	+ 3.55
	55.5	dolomite (prismatic dolospar)	- 9.91	+ 4.97

Table 1. Isotope compositions ($\delta^{13}C$ y $\delta^{18}O$) of carbonate host-rock samples of the Salmerón upper sulfur body, Las Minas de Hellín basin, MINERSA boreholes.

Tabla 1. Composición isotópica ($\delta^{13}C$ y $\delta^{18}O$) de los carbonatos huésped del nivel mineralizado superior de Salmerón, cuenca de Las Minas de Hellín, sondeos MINERSA.

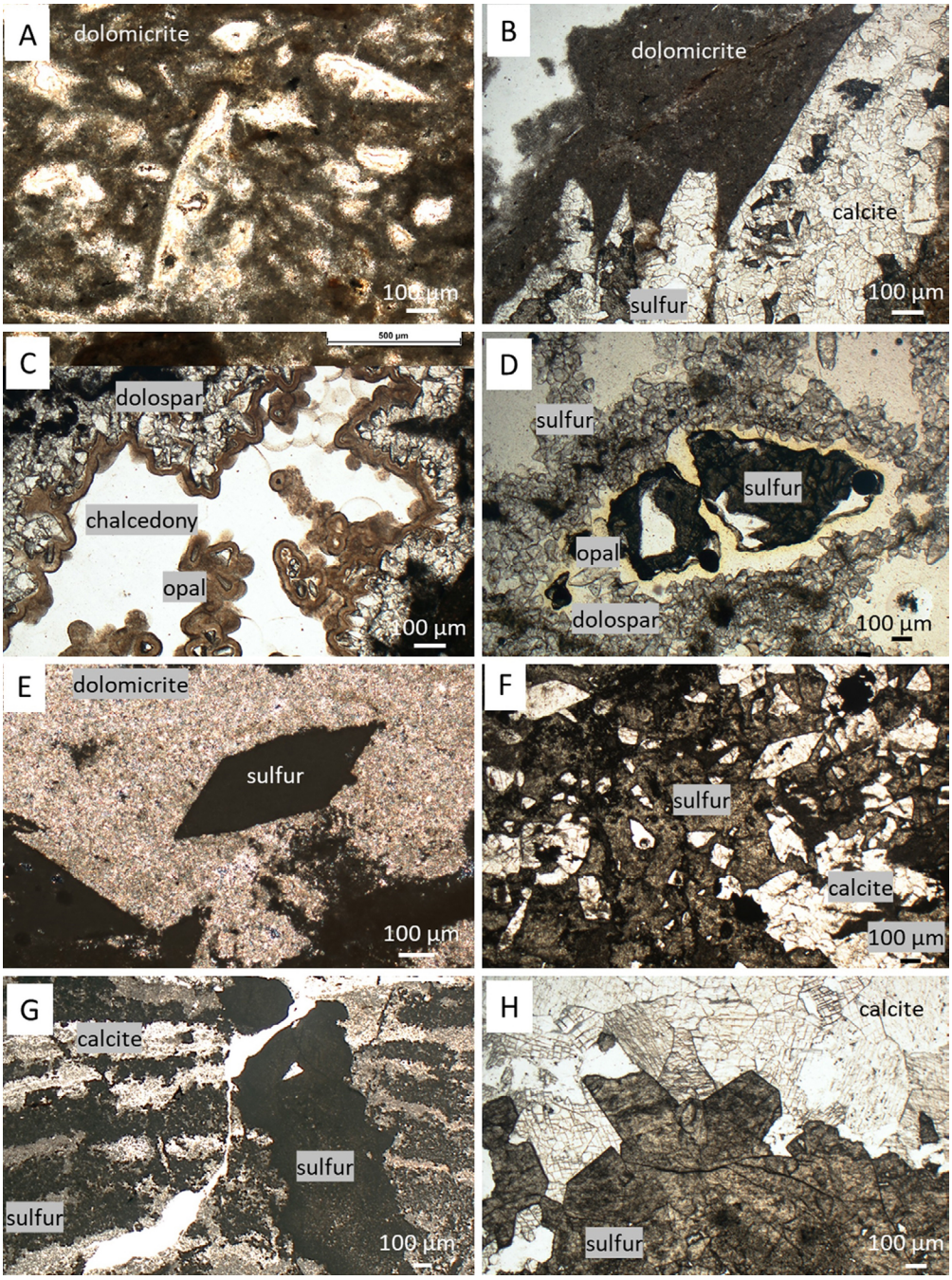

Figure 10. Petrographic microscope images of the Salmerón USB (Las Minas de Hellín basin). A) Peloidal dolomicrite with gypsum casts filled by opal and chalcedony (HE13-67.0 m; PPL). B) Peloidal dolomicrite with gypsum casts filled by calcite and native sulfur (HE1-63.7 m; XPL). C) Prismatic (scalenohedral) dolospar crystals, opal lepispheres and chalcedony filling voids in a dolomicrite matrix (HE19-56.6 m; PPL). D) Prismatic (scalenohedral) dolospar and native sulfur filling pseudomorphs after gypsum (HE19-56.6 m; PPL). E) Sulfur pseudomorphs after gympsum in a prismatic dolomicrite matrix (HE14-46.3 m; XPL). F) Native sulfur and sparry calcite filling fractures (HE1-66.1 m; XPL). G) Native sulfur vein crosscutting laminated dolomicrite. Diatomite-rich layers cemented by sulfur and calcite (HE1-63.7 m; PPL). H) Native sulfur and sparry calcite filling fractures (HE1-63.7 m; PPL).

Figura 10. Imágenes de microscopía óptica del nivel mineralizado superior de Salmerón (cuenca de Las Minas de Hellín). A) Dolomicrita peloidal con moldes de yeso rellenos de ópalo y calcedonia (HE13-67,0 m; PPL). Dolomicrita peloidal con moldes de yeso rellenos de calcita y azufre elemental (HE1-63,7 m; XPL). C) Doloesparita escaleonoédrica, lepisferas de ópalo, y calcedonia rellenando cavidades (HE19-56,6 m; PPL). D) Doloesparita escaleonoédrica y azufre elemental pseudomorfizando yeso (HE19-55,6 m; PPL). E) Pseudomorfos de yeso reemplazados por azufre elemental en una matriz de dolomicrita (HE14-46,3 m; XPL). F) Azufre elemental y calcita esparítica rellenando fracturas (HE1-66,1 m; XPL). G) Venas de azufre elemental cortando láminas de dolomita y diatomeas. Azufre y calcita cementan láminas diatomíticas (HE1-63,7 m; PPL). H) Azufre elemental y calcita esparítica rellenando fracturas (HE1-63,7 m; XPL).

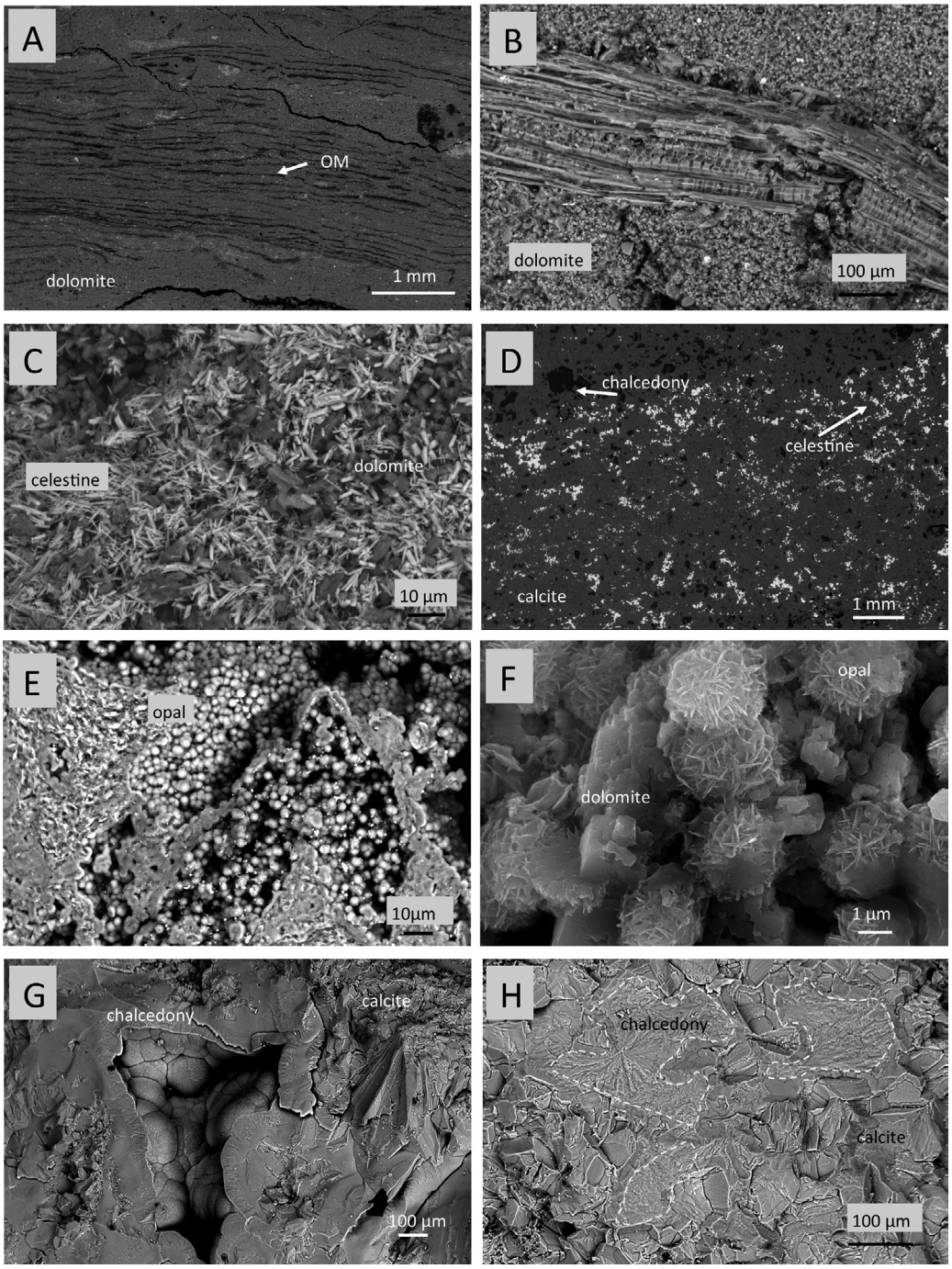

Figure 11. Celestine and organic and siliceous components in the Salmerón USB (Las Minas de Hellín basin). A) Organic matter distribution into dolomicrite layers (HE14-46.3 m; SEM-BSE). B) Plant remains (phytolits) in a dolomicrite layer (HE14-45.0 m; SEM-BSE). C) Acicular celestine crystals scattered in a dolomicrite layer (HE1-67.2 m; SEM-BSE). D) Celestine crystals drawing calcite pseudomorphs after gypsum. Calcite and chalcedony replace the original dolomite layer (HE14-47.6 m; SEM-BSE). E) Lepispheres of opal lining empty gypsum casts (HE13-68.6 m; SEM-BSE). F) Opal lepispheres (HE14-46.5 m; FESEM-SE). G) Chalcedony filling open voids (gypsum casts and veins) in a calcified dolomite layer (HE14-56.6 m; SEM-BSE). H) Sparry calcite and chalcedony replacing a dolomite layer (HE14-56.6 m; SEM-BSE).

Figura 11. Celestina y componentes orgánicos y silíceos en la roca huésped del nivel mineralizado superior de Salmerón (cuenca de Las Minas de Hellín). A) Distribución de láminas ricas en materia orgánica entre láminas de dolomicrita (HE14-46,3 m; SEM-BSE). B) Fitolitos en una lámina de dolomicrita (HE14-45,0 m; SEM-BSE). C) Cristales aciculares de celestina en una lámina de dolomicrita (HE1-67,2 m; SEM-BSE). D) Cristales de celestina perfilando pseudomorfos de yeso reemplazados por calcita. Calcita y calcedonia reemplazan láminas originales de dolomita (HE14-47,6 m; SEM-BSE). E) Lepisferas de ópalo tapizando moldes huecos de yeso (HE13-68,6 m; SEM-BSE). F) Lepisferas de ópalo (HE14-46,5 m; FESEM-SE). G) Calcedonia rellenando cavidades (moldes de yeso y venas) en una lámina dolomítica (HE14-56,6 m; SEM-BSE). H) Calcita esparítica y calcedonia reemplazando una lámina de dolomita (HE14-56,6 m; SEM-BSE).

Marked isotope differences exist for each carbonate mineral. Aragonite show positive $\delta^{13}C$ (between 2.63 and 3.71‰) and $\delta^{18}O$ (between 5.85 and 6.06‰) values. Calcites, on the contrary, characterize by negative $\delta^{13}C$ (between -5.64 and -4.40‰) and $\delta^{18}O$ (between -8.34 and -7.22‰) values. The three dolomite types exhibit negative $\delta^{13}C$ (between -9.91 and -4.54‰) but positive $\delta^{18}O$ (between 2.77 and 9.92‰) compositions. The values obtained are within the range of those previously published for the upper carbonate unit in Las Minas de Hellín (Servant-Vidary *et al*., 1990; Lindtke *et al*., 2011), in the equivalent unit in the Cenajo basin (Bellanca *et al*., 1989), and in the underlying evaporite unit in Las Minas de Hellín basin (Ortí *et al*., 2014b; Pineda *et al*., 2021).

5. Discussion

5.1. Paragenetic sequence

Discerning whether the elemental sulfur deposit of Las Minas de Hellín is biosyngenetic or bioepigenetic is not straightforward. Both, the sedimentary and the diagenetic realms, can produce biochemical conditions for hydrogen sulfide generation and subsequent oxidation to sulfur.

Based on petrographic observations, the primary mineral association in the Salmerón USB consists mainly of dolomicrite, silica skeletons (diatoms), and gypsum, and to a lesser extent, aragonite. Aragonite and dolomicrite are subaqueous precipitates whereas lenticular gypsum grew interstitially in the unconsolidated sediment. Distribution of disseminated celestine, following sedimentary laminations, points to a primary origin precipitating directly from the coastal lake waters or into the unconsolidated sediment.

Dolomite is, by far, the most abundant sedimentary component. There is no evidence of any mineral precursor of dolomite. The empty cores of the dolomicrite crystals (Figures 8A, 8B and 8C) point to a microbial mediated nucleation. Bacterially mediated dolomite precipitation has been documented in both anaerobic and aerobic modern sedimentary environments (Vasconcellos and McKenzie, 1997; Warthmann *et al*., 2000, Sánchez-Román *et al*., 2009, 2011). After equant dolomicrite nucleation, crystals can continue growing in the prismatic dolomicrite habit (figures 8D and 8E).

Precipitation of dolomicrite and aragonite containing abundant plant remains (subsequently degraded to S-rich organic matter) alternate with short periods of highly accumulation of siliceous remains (diatoms, golden-brown algae, sponges) showing a varve-like lamination.

Diatom-rich layers in Las Minas de Hellín basin was originally interpreted as related to the contemporaneous lamproitic volcanism of the Monagrillo volcano (Elízaga, 1994), later to episodic events of water stagnation (Servant-Vildary *et al*., 1990), and recently to cyclic increase of nutrient supplies triggering diatomite blooms (Ortí *et al*., 2014b). None of these interpretations seem conclusive. The abundance of diatomite organism in the water column and their preservation in sediments are not directly related. After dying, most diatom valves dissolve in water before reaching the basin floor. Their abundance in sediments depend on the chemical conditions of waters (pH, temperature, ionic strength), physical characteristics of the basin (meromixis, water body permanence), biological interactions (bacterial mineral dissolution), and sediment conditions (grazing and fecal pelletization, organic content) (Lewin, 1961; Barker *et al*., 1994; Bidle and Azam, 1999; Bidle *et al*., 2002).

The paragenetic sequence of the Salmerón USB, differentiating between sedimentary and diagenetic realms, is summarized in Figure 12. Unlike in the underlying evaporitie unit, gypsum in the mineralized lower part of the upper carbonate unit does not show subaqueous lithofacies as described in Ortí *et al*. (2014b). Gypsum is restricted to disseminated lenticular crystals (now empty casts or sulfur and/or calcite pseudomorphs) showing evidence of displacive growth into the dolomicrite matrix.

Dolospar, elemental sulfur, opal, chalcedony and calcite are diagenetic phases. All of them formed after sediment lithification and dissolution of interstitial gypsum. Idiomorphic dolospar and opal lepispheres consist of early cements lining the inner walls of the empty gypsum casts. Later, elemental sulfur, chalcedony and sparry calcite fill the gypsum casts, veins and fractures. The crystallization order between these diagenetic minerals is unclear because they seem to be contemporaneous although calcite and chalcedony frequently replace native sulfur.

In the base of the ore body, dolostones are fully replaced by the end members of the paragenetic sequence, calcite and silica (chert). Mineralogical and petrological characteristics of this basal part are similar to those described by Pozo *et al*.

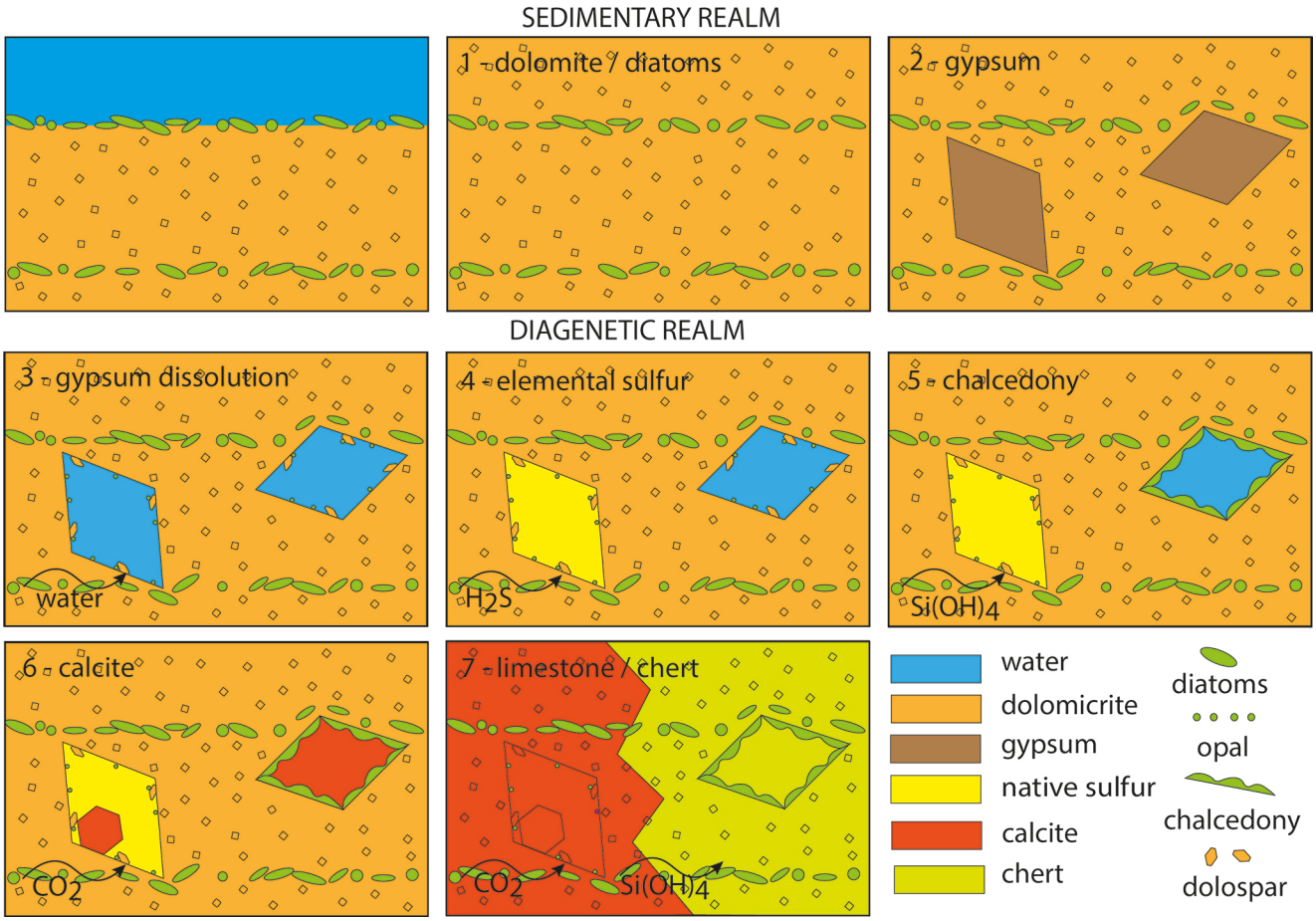

Figure 12. Paragenetic sequence of the Salmerón USB (Las Minas de Hellín basin). 1) Sedimentary deposition of biomediated dolomicrite and diatomite, organich-rich layers. 2) Synsedimentary interstitial growth of gypsum crystals. 3) Dissolution of gypsum in a partially lithified sediment (early diagenesis). Prismatic dolospar crystals and opal lepispheres lining empty gypsum casts. 4) Native sulfur filling pseudomorphs after gypsum. 5) Chalcedony filling pseudomorphs. 6) Calcite filling pseudomorphs and replacing native sulfur. 6) Complete calcification and silicification (chert) of the host rock (included native sulfur).

Figura 12. Secuencia paragenética del nivel mineralizado superior de Salmerón (cuenca de las Minas de Hellín). 1) Acumulación sedimentaria de láminas de dolomicrita biomediada, diatomeas y materia orgánica. 2) Crecimiento intersticial de cristales de yeso en el sedimento. 3) Disolución del yeso en el sedimento parcialmente litificado (diagénesis temprana). Doloesparita y lepisferas de ópalo tapizan los moldes de yeso. 4) Azufre elemental rellena cavidades y pseudomorfiza yeso. 5) Calcedonia rellena cavidades. 6) Calcita pseudomorfiza yeso y reemplaza azufre elemental. 7) Silicificación y calcificación completa de la roca huésped (incluido el azufre).

(2016) for the 'carbonate and silica-rich mounds' outcropping 1km north of the studied Salmerón USB (Figure 3). These structures have been interpreted as thermal spring deposits related to fissures. Indeed, some of their pictures of large voids filled by calcite probably correspond to empty casts and pseudomorphs after gypsum.

5.2. Sulfate isotope geochemistry (bibliographic data)

Several studies have analyzed the sulfate isotope compositions ($\delta^{34}S$ and $\delta^{18}O$) of primary gypsum (sedimentary), secondary gypsum (after anhydritization), elemental sulfur occurrences, and diagenetic gypsum from Las Minas de Hellín and the Cenajo basins (Servant-Vildary *et al.*, 1990; Lindtke *et al.*, 2011, Ortí *et al.*, 2014b; Pineda *et al.*, 2021). Sulfate isotopic signatures have been used to propose a syngenetic origin for the native sulfur occurrences (Figure 13). Although primary gypsum is not preserved in the Salmerón USB, these previously published data provided a framework for our interpretations.

Sulfur isotope compositions group around two clusters (Figure 13): (1) positive $\delta^{34}S$ values in primary/secondary gypsum, and (2) negative $\delta^{34}S$ values in elemental sulfur and diagenetic gypsum. Synsedimentary gypsum (including primary and secondary gypsum after anhydrite) shows a wide

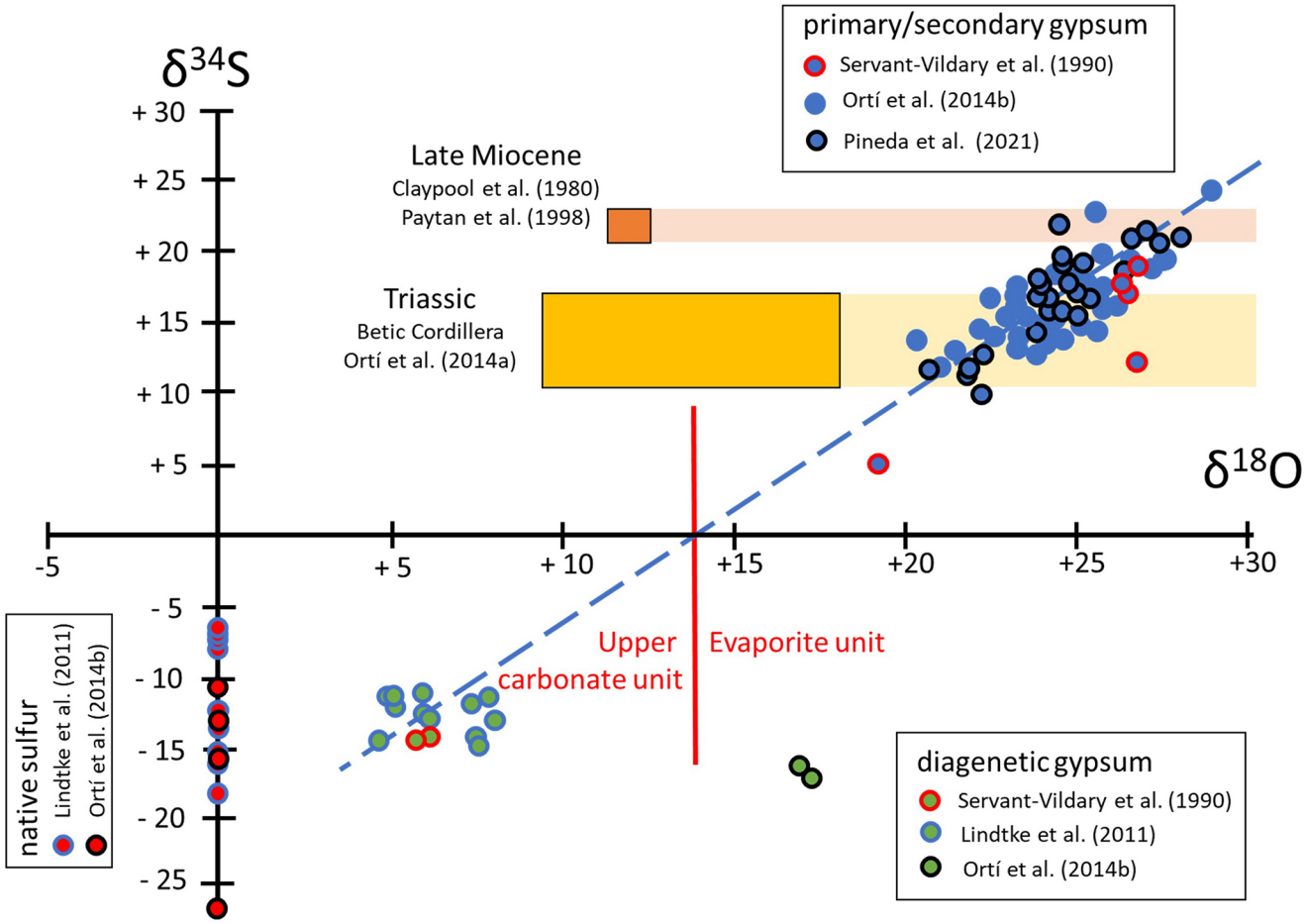

Figure 13. Bibliographic sulfur and gypsum sulfate isotope ($\delta^{34}S$ and $\delta^{18}O$) data from Las Minas de Hellín and the Cenajo basins. Sedimentary and diagenetic gypsum data from Servant-Vildary *et al.* (1990) are unlocated in the lithostratigraphic succession. Sulfur and diagenetic gypsum data from Lindtke *et al.* (2011) belong to the USB (upper carbonate unit). Data of primary and secondary gypsum (after anhydrite) from Ortí *et al.* (2014) and Pineda *et al.* (2021) correspond to the evaporite unit, whereas of elemental sulfur are unlocated.

Figura 13. Datos bibliográficos de la composición isotópica del azufre y del sulfato en yeso ($\delta^{34}S$ and $\delta^{18}O$) en las cuencas de Las Minas de Hellín y del Cenajo. Los datos de yesos sedimentarios y diagenéticos de Servant-Vildary *et al.* (1990) corresponden a muestras sin situación litoestratigráfica. Los datos de azufre elemental y yeso diagenético de Lindtke *et al.* (2011) corresponden al nivel mineralizado superior (unidad carbonatada superior). Los datos de yeso primario y secundario (después de yeso) de Ortí *et al.* (2014) y de Pineda *et al.* (2021) corresponden a la unidad evaporítica, sin embargo, las muestras de azufre no tienen posición estratigráfica.

range of $\delta^{34}S$ values, ranging between those expected for continental waters recycling Triassic evaporites ($\delta^{34}S$ ~ 12 to 17‰, Ortí *et al.*, 2014a) abundant in the drainage area, and those expected for Late Miocene seawater ($\delta^{34}S$ ~ 21‰, Claypool *et al.*, 1980; Paytan *et al.*, 1998). Recurrent seawater inputs are supported by marine assemblages of diatoms (Servant-Vildary *et al.*, 1990), foraminifera, radiolarians, sponges, silicoflagellates and dinoflagellates (Pineda *et al.*, 2021).

Although $\delta^{34}S$ data in synsedimentary gypsum could be explained by mixing of continental and marine inputs, this is not the case for the $\delta^{18}O$ enrichments, of up to 20‰, reported in the evaporite unit. All authors agree that isotopic enrichments in both $\delta^{34}S$ and $\delta^{18}O$ of synsedimentary gypsum were mediated by bacterial sulfate reduction processes (Servant-Vildary *et al.*, 1990; Lindtke *et al.*, 2011; Ortí *et al.*, 2014b; Pineda *et al.*, 2021).

However, Lindtke *et al.* (2011) propose a biosyngenetic origin for the sulfur occurrences in Las Minas abandoned quarries, based on: (1) the isotopic $\delta^{34}S$ and $\delta^{18}O$ enrichments in sedimentary gypsum previously reported by Servant-Vildary *et al.* (1990), (2) the formation of biomediated dolomicrites, and (3) the bending of sediment layers around sulfur nodules. In our opinion, this interpretation is not well founded because: (1) there is not sedimentary gypsum in Las Minas quarries,

(2) biomediated dolomite is ubiquitous in the complete Miocene succession, and (3) sediment laminar deformation by the interstitial growth of different minerals is characteristic of early diagenetic processes.

Interestingly, Lindtke *et al*. (2011) recognize that most of the gypsum in Las Minas quarries is diagenetic in origin. In fact, their images of sulfur occurrences in Las Minas correspond to discrete disseminations of native sulfur formed within diagenetic (satin-spar) gypsum, and into bedding-parallel joints in carbonate beds. They also report images of centimetric sulfur nodules formed within dolomicrite beds in the Cenajo basin (not present in Las Minas) where primary gypsum is absent.

The average depletion of 30‰ in $\delta^{34}S$ between synsedimentary gypsum and native sulfur reported by Lindtke *et al*. (2011) (Figure 13) is within the isotopic fractionation range expected after bacterial sulfate reduction processes. However, the biomediated fractionation leading to the observed isotopic depletion in elemental sulfur could have taken place during sedimentation (syngenetic) or after (diagenetic). Although all authors suggest a contemporaneity between synsedimentary gypsum and the formation of elemental sulfur, their data cannot prove it. All reported isotopic data from sedimentary gypsum (Servant-Vildary *et al*., 1990; Ortí *et al*., 2014b; Pineda *et al*., 2021) belongs to the evaporite unit, whereas isotopic data from elemental sulfur (Lindtke *et al*., 2011; Ortí *et al*., 2014b) corresponds to the USB in the overlying upper carbonate unit.

Microbial sulfate reduction, hydrogen sulfide, and the subsequent formed native sulfur, can occur in both sedimentary (biosyngenetic) and diagenetic (bioepigenetic) realms. Our observations in the Salmerón USB show evidence that native sulfur in the USB postdate primary gypsum and dolomicrite formation in the sedimentary environment, and even the dissolution of the former.

$\delta^{34}S$ values of diagenetic gypsum match with those of related native sulfur suggesting no fractionation during the oxidation process. However, differences exist in sulfate-$\delta^{18}O$ values. $\delta^{18}O$ in diagenetic gypsum of the USB (Servant-Vildary *et al*., 1990; Lindtke *et al*., 2011) are lower than those observed in the LSB (Ortí *et al*., 2014b). Accurate petrologic and geochemical studies are required in order to interpret the mineralogenetic relations between diagenetic gypsum and elemental sulfur in each sulfur body.

5.3. Carbonate isotope geochemistry

Previous works in Las Minas de Hellín and the Cenajo basins agree with a primary (sedimentary) origin for dolomicrite beds in both the evaporite unit and in the lower part of the upper carbonate unit. However, some differences exist with respect the interpretation of calcite origin.

We compare our values from the Salmerón USB (Figure 14A) with those reported for the (1) Mobarque carbonate mound (Pozo *et al*., 2016) (Figure 14B); (2) Maeso, U1 and U2 carbonate mounds (Pozo *et al*., 2016) (Figure 14C); (3) evaporite unit in Las Minas de Hellín (Ortí *et al*., 2014b; Pineda *et al*., 2021) (Figure 14D); (4) lower part of the upper carbonate unit in Las Minas de Hellín (Servant-Vildary *et al*., 1990; Lindtke *et al*., 2011) and Cenajo basins (Bellanca *et al*., 1989) (Figure 14F).

Overall, our data match with previous ones, reporting positive $\delta^{13}C$ and $\delta^{18}O$ values in aragonite, negative $\delta^{13}C$ and $\delta^{18}O$ in calcite, and negative $\delta^{13}C$ but positive $\delta^{18}O$ in dolomite. However, some methodological and interpretative aspects require discussion.

The Mobarque carbonate mound correlates stratigraphically with the studied Salmerón USB. This positive relief is located only 1km north of the sulfur-bearing boreholes (Figure 2). According to Pozo *et al*. (2016), two types of dolomite are distinguished in this carbonate mound, primary dolomicrite which is the main component in massive dolostones, and aggrading neomorphic dolospar accompanying dolomicrite in laminated dolomite lithofacies. Isotopic data reported for laminated dolomites in the Mobarque carbonate mound (Figure 14B) show intermediate values, between diagenetic calcite and massive dolomite (primary dolomicrite) end-members. As $\delta^{13}C$ values are always negative and similar for both minerals, the intermediate values are only distinguished by $\delta^{18}O$. Similar intermediate values have been also reported in Las Minas de Hellín abandoned quarries (lower part of the upper carbonate unit) by Lindtke *et al*. (2011) (Figure 14E) and interpreted as mixing of calcite and dolomite. The hydrothermal origin for dolomite suggested by Pozo *et al*. (2016) is discussed below.

A marked difference in $\delta^{18}O$ exists between positive values in dolomicrites and aragonites and negative values in calcites. All authors interpret the positive $\delta^{18}O$ values in dolomicrites as formed from highly evaporated lake waters. Less positive

$\delta^{18}O$ values in aragonites (Figure 14F) are interpreted by Bellanca *et al*. (1989) as the early primary precipitation of this mineral, with respect to dolomite, in relatively less concentrated waters.

All authors agree on calcite resulting from the precipitation in meteoric-derived diagenetic waters (Lindtke *et al*., 2011; Ortí *et al*., 2014b; Pozo *et al*., 2016).

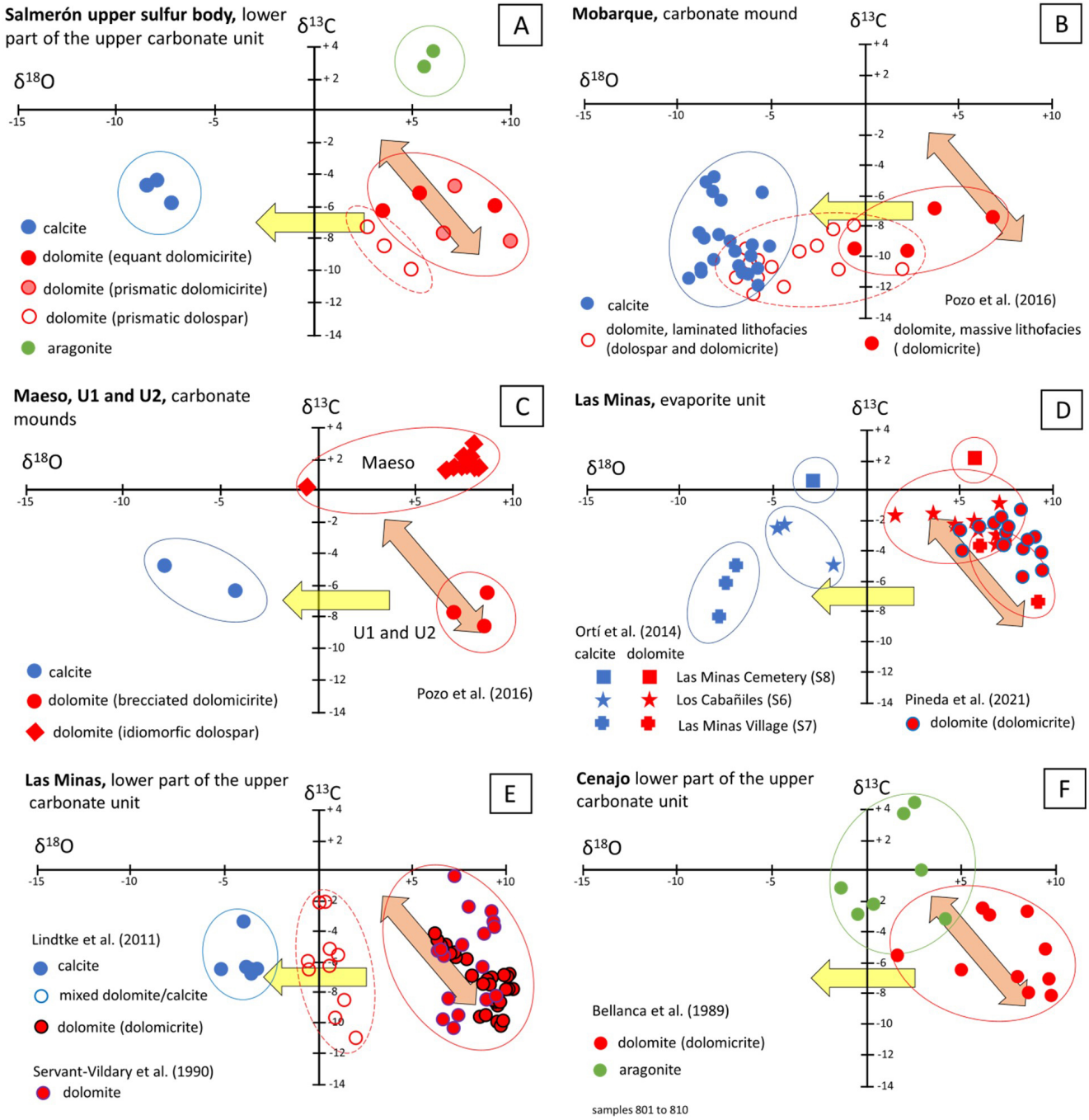

Figure 14. Carbonate isotope ($\delta^{13}C$ and $\delta^{18}O$) data from Las Minas de Hellín and the Cenajo basins. A) New data from the Salmerón USB. B) Data from the Mobarque carbonate mound (Pozo *et al*., 2016). C) Data from the U1, U2 and Maeso carbonate mounds (Pozo *et al*., 2016). D) Data from the evaporite unit in Las Minas de Hellín basin (Ortí *et al*., 2014; Pineda *et al*., 2021). E) Data from the upper carbonate unit in Las Minas de Hellín (Servant-Vildary *et al*., 1990; Lindtke *et al*., 2011). F) Data from the upper carbonate unit in the Cenajo basin (Bellanca *et al*., 1989).

Figure 14. Composición isotópica de los carbonatos ($\delta^{34}S$ and $\delta^{18}O$) de las cuencas de Las Minas de Hellín y del Cenajo. A) Nuevos datos de la roca huésped del nivel mineralizado superior de Salmerón. B) Datos del montículo carbonatado de Mobarque (Pozo *et al*., 2016). Datos de los montículos carbonatados U1, U2 y Maeso (Pozo *et al*., 2016). D) Datos de la unidad evaporítica en Las Minas de Hellín (Ortí *et al*., 2014b; Pineda *et al*., 2021). E) Datos de la unidad carbonatada superior en Las Minas de Hellín (Servant-Vildary *et al*., 1990; Lindtke *et al*., 2011). F) Datos de la unidad carbonatada superior en el Cenajo (Bellanca *et al*., 1989).

Most $\delta^{13}C$ values in sedimentary dolomicrites are negative. These negative values related to spheroidal dolomicrite habits have been interpreted as microbial induced precipitation of dolomite, on the lake floor, by remineralization of the CO_2 released during organic matter degradation (Bellanca *et al*., 1989; Servant-Vildary *et al*., 1990). Based on the presence of native sulfur in Las Minas de Hellín quarries, Lindtke *et al*. (2011) suggest that H_2S and CO_2 were formed from organic matter degradation by SRB. Subsequently dolomicrite precipitated due to the increase in pH and alkalinity, and H_2S was oxidized to S^0, most probably by SOB.

A negative correlation between $\delta^{13}C$ and $\delta^{18}O$ in dolomicrite samples of Las Minas de Hellín quarries (Figure 14E) is originally reported by Lindtke *et al*. (2011): the most ^{18}O-enriched and the most ^{13}C-depleted dolomites. According to these authors, the stages of higher evaporation and saline concentration (^{18}O-enriched) are also the most active for bacterial remineralization of organic matter (^{13}C-depleted). Similar trends can be recognized in the data reported for the evaporite unit (Ortí *et al*., 2014b; Pineda *et al*., 2021) (Figure 14D), and in the lower part of the upper carbonate unit in the Cenajo basin (Bellanca *et al*., 1989) (Figure 14F).

In conclusion, there is a general agreement interpreting carbonates in both the evaporite unit and in the lower part of the upper carbonate unit. The positive $\delta^{13}C$ and $\delta^{18}O$ values in sedimentary aragonite point to less concentrated, mainly marine waters. The negative $\delta^{13}C$ values in sedimentary dolomites are due to remineralization of organic matter. The positive $\delta^{18}O$ in sedimentary dolomites indicate highly evaporation conditions. Calcite is a diagenetic mineral showing negative $\delta^{13}C$ (precursor dolomite) and negative $\delta^{18}O$ (meteoric derived waters).

5.4. Silicified carbonate mounds

A different interpretation of carbonate isotope data is suggested by Pozo *et al*. (2016) for their 'carbonate mounds'. These authors admit that such morphological ridges are clearly distinctive from the carbonate mounds usually described in the geological literature (e.g., tufa, travertine, mud-mound carbonates). They conclude that such carbonate mounds in Las Minas de Hellín are related to local artesian seepage and relatively high temperatures.

In the Mobarque, U1 and U2 silicified carbonate mounds, located close to the Salmerón and Las Minas USB (Figure 2), the negative $\delta^{13}C$ values in both massive and laminated dolomite lithofacies (Figure 14B) are interpreted by Pozo *et al*. (2016) as due to the contribution of depleted $\delta^{13}C$, hydrothermal CO_2-rich waters.

According to Pozo *et al*. (2016), depleted $\delta^{13}C$ hydrothermal CO_2 dominates close to the thermal discharging points. Then, the progressive 'degassing´ (escape of hydrothermal CO_2) increases the $\delta^{13}C$ of the remaining CO_2 in water and in the neoformed dolomites (Figure 14C). The Maeso mound (Figure 2) is characterized to be poorly affected by silicification, shows a clastic appearance with gravels and cross beddings, contains abundant void-filling dolospar overcoming primary dolomicrite, and exhibits sedimentary bedding containing abundant bioclastic and organic remains (Pozo *et al*., 2016). Unlike the other carbonate mounds interpreted as formed at subsurface, the Maeso is interpreted as a subaqueous deposit. While in the Mobarque, U1 and U2 carbonate mounds, the hydrothermal CO_2 was released in a confined system, without significant fractionation by degassing, in the Maeso mound, the thermal waters rose to the lake floor and most of the isotopically lower $\delta^{13}C$ hydrothermal CO_2 escaped by degassing. According to this model, dolospar in the Maeso should be less influenced by hydrothermal waters although no specific mechanism is suggested for its genesis.

The Maeso mound is in the elevated northern block of the Mobarque fault (Figure 2). The Mobarque, U1 and U2 silicified carbonate mounds, the studied Salmerón USB, and the abandoned mined area of las Minas, are all of them nearby and located in the southern sunken block. In our opinion, the geochemical and mineralogical processes occurred in the Mobarque-Salmerón-Las Minas area were strongly related to the hydrothermal activity along the Mobarque fault. These conditions could be different to those occurred in the further away Maeso area.

The positive $\delta^{13}C$ and $\delta^{18}O$ values of de Maeso dolospar match the compositions of primary aragonite (figures 14 and 14F), and of some dolomicrite beds (Figure 14D). These positive $\delta^{13}C$ and $\delta^{18}O$ values have been interpreted as diagnostic of poorly concentrated, and less affected by biogenic organic matter degradation, lake waters (perhaps even marine). The lake water dilution mechanism by increasing freshwater or seawater

inputs, suggested by Bellanca *et al*. (1989) and Ortí *et al*. (2014b), for these positive isotope data, is in accordance with the hydrothermal groundwater mechanism proposed by Pozo *et al*. (2016). Dolospar formed by aggrading neomorphism in the distal Maeso area should have occurred with minor or without contribution of hydrothermal CO_2.

Petrographic descriptions of the carbonate mounds provided by Pozo *et al*. (2016) are coincident with the host rock of the Salmerón USB. The intermediate $\delta^{18}O$ values, with gradual variation from heavier to lighter compositions in the dolospar of the Mobarque mound (yellow arrow in Figure 14B), and the negative $\delta^{18}O$ values in calcites, are interpreted as progressive dilution of thermal waters. Dolospars formed far from the hydrothermal vents record higher $\delta^{18}O$ values more influenced by the lake waters or confined brines. Conversely, dolospars formed close to the hydrothermal vents are less affected by dilution with lake waters, or confined brines, recording lower $\delta^{18}O$ values, characteristic from the hydrothermal source.

Our dolospar data (Figure 14A) match with values in the Mobarque dolospar trend towards lighter $\delta^{18}O$ compositions. The hydrothermal interpretation of Pozo *et al*. (2016) for neomorphic dolospar in the Mobarque seepage mound can be extended to the prismatic dolospar lining voids in the stratigraphically equivalent, but less affected by hydrothermal silicification, Salmerón USB.

5.5. Bioepigenetic model for the USB in Las Minas de Hellín basin

The native sulfur occurrences in the studied boreholes, consisting of pseudomorphs after gypsum and veins filling fractures, must be considered as early diagenetic. Preservation of pseudomorphs after gypsum requires a certain degree of lithification. The observed replacement of gypsum by elemental sulfur is preceded by the complete dissolution of gypsum maintaining uncollapsed gypsum casts. Based on these observations we consider the Salmerón USB as epigenetic in origin. Time lags between deposition of the hosting sediment, precipitation of interstitial primary gypsum, and the subsequent dissolution and replacement by native sulfur could be short but cannot be determinated.

The bioepigenetic model for the Salmerón USB includes the dissolution of gypsum, the organic matter degradation and the bacterial sulfate reduction of dissolved sulfate resulting in the generation of the H_2S which was subsequently oxidized to native sulfur precipitating in empty voids (mainly gypsum casts), veins, and fractures, and with minor extension, growing in a displacive way or cementing diatom-rich layers.

Intense brecciation, silicification and calcification of the host rock in the Salmerón USB are similar features than those described for the nearby and contemporaneous Mobarque, U1 and U2 carbonate mounds interpreted as related to hydrothermal seepage waters (Pozo *et al*., 2016). A hydrothermal origin, or contribution, in the dissolution of primary gypsum and in the genesis of the elemental sulfur cannot be ruled out.

We interpret the native sulfur occurrences of the USB hosted in the base of the upper carbonate unit in Mobarque, Las Minas de Hellín quarries and in the Cenajo areas, as early diagenetic in origin. Unlike in Salmerón, which contains primary gypsum and is affected by hydrothermal calcification and silicification, the relationship of these sulfur occurrences with fibrous satin spar gypsum in diastems and fractures, and the development of sulfur nodules in carbonates and conglomerates without evidence of primary gypsum precipitation, suggests a certain degree of transport of dissolved sulfate towards organic-rich unlithified sediments were native sulfur and diagenetic gypsum formed within sulfuretums.

6. Conclusions

Two economically elemental sulfur bodies (more than 15% of S^0) were exploited in Las Minas de Hellín basin. The USB is hosted by dolomites and diatom-rich beds of the upper carbonate unit (Calvo *et al*., 2014). This deposit was exploited in small galleries in the Mobarque and Salmerón areas of Las Minas de Hellín basin, as well as in the Cenajo basin. Sulfur occurrences outcropping in Las Minas de Hellín abandoned quarries also belongs to the USB. All previous published information about elemental sulfur in Las Minas and the Cenajo basins are limited to this USB (Bellanca *et al*., 1989; Servant-Vildary *et al*., 1990; Lindtke *et al*., 2011, Ortí *et al*., 2014b; Pineda *et al*., 2021).

The LSB, extensively exploited in underground mines in Las Minas de Hellín, is hosted by gypsum and corresponds to the evaporite unit (Calvo *et al*., 2014). Minor occurrences of elemental sulfur can be recognized in barren gypsum levels

outcropping in the Barranco de los Hinojos, further from underground mine operations. To date the LSB has not been interpreted.

In the Salmerón area, close to the Mobarque fault and to the hydrothermal carbonate mound described by Pozo *et al*. (2016), elemental sulfur of the USB fill pseudomorphs after gypsum as well as fissures and bed joints. Calcite and silica (opal and chalcedony) can replace both elemental sulfur and dolomite matrix. Native sulfur mineralization must be considered as bioepigenetic because postdates the authigenic interstitial growth of primary gypsum and its subsequent dissolution, leading to formation of empty casts, in a partially lithified sediment.

In Las Minas abandoned quarries and in the Mobarque area, little further away from the seepage carbonate mound, the host rock of the USB does not contain primary gypsum neither pseudomorphs. In Mobarque, as in the neighboring the Cenajo basin, elemental sulfur occurs as nodules grown in a non-completely lithified dolomite matrix. In Las Minas quarries, most of the native sulfur occurs with diagenetic gypsum (satin spar) in bed joints and fissures. We do not found evidence of a biosyngenetic origin for elemental sulfur in these areas.

Summarizing, the USB in Las Minas and the Cenajo basins, hosted in the base of the upper carbonate unit, is considered as bioepigenetic. From the mineralogenetic point of view, elemental sulfur formed within incompletely lithified sediments during early diagenesis, at the same time that further carbonate muds (dolomite and aragonite) deposited in the basin floor. Although from the sedimentological point of view the elemental sulfur can be considered as contemporaneous with sedimentation, from the mineralogenetic view, the elemental sulfur postdates its hosting matrix.

This textural and paragenetic SEM-EDS work represent a case study that can be illustrative for future research in sulphur deposits in order to clarify the biosyngenetic/bioepigenetic character of a deposit and to guide stable isotopy sampling strategies of the concerned mineral phases.

Acknowledgments

This study was provided by the Spanish Government Projects CGL-2016-79458 and PID2020-118999GB-I00, and by the Catalonian Government Action 21-SGR-829. The authors are indebted to the Instituto de Estudios Albacetenses providing grant funds (1994) which allowed the recovery of borehole cores and lost documents of the ancient mining company.

References

Anadón, P., Rosell, L., and Talbot, M. R. (1992). Carbonate replacement of lacustrine gypsum deposits in two Neogene continental basins, eastern Spain. Sedimentary Geology, 78, 201-216.

Barker, J., Cochran, D., and Semrad, R. (1979). Economic geology of the Mishraq native sulfur deposit, northern Iraq. Economic Geology, 74, 484-495.

Barker, P., Fontes, J. C., Gasse, F., and Druart, J. C. (1994). Experimental dissolution of diatom silica in concentrated salt solutions and implications for paleoenvironmental reconstruction. Limnology and Oceanography, 39, 99-110.

Baas Becking, L. (1925). Studies on the sulphur bacteria. Annals of Botany, 39, 613-650.

Bellanca, A., Calvo, J. P., Censi, P., Elízaga, E., and Neri, R. (1989). Evolution of diatomite-carbonate lacustrine cycles of Miocene age, Southeastern Spain: petrology and isotope geochemistry. Journal of Sedimentary Petrology, 59, 45-52.

Bellon, H., Bizon, G., Calvo, J. P., Elízaga, E., Gaudant, J., and López, N. (1980). Le volcán du Cerro Monagrillo (Province of Murcia): age radiométrique et corrélations avec les sédiments néogènes du bassin de Hellín (Espagne). Comtes Rendus de l'Académie des Sciences, Série 2, Mécanique Physique, Chimie, Sciences de l'Univers, Sciences de la Terre, 292, 1035-1038.

Berner, R. A. (1980). Early Diagenesis. In: D. H. Holland (ed.), A theoretical approach. Priceton University Press, 241 pp.

Bidle, K. D., and Azam, F. (1999). Accelerated dissolution of diatom silica by marine bacterial assemblages. Nature, 397, 508-512.

Bidle, K. D., Maganelli, M., and Azam, F. (2002). Regulation of oceanic silicon and carbon preservation by temperature control on bacteria. Science, 298, 1980-1984.

Böttcher, M. E., and Parafiniuk, J. (1998). Methane-derived carbonates in native sulfur deposits: stable isotope and trace element discrimination related to the transformation of aragonite to calcite. Isotopes in Environmental and Health Studies, 34, 177-190.

Brookins, D. G. (1988). Eh-pH diagrams for geochemistry. Springer-Verlag, Berlin, 190 pp.

Calvo, J. P., Elízaga, E., López, N., Robles, F., and Usera, J. (1978). El Mioceno superior continental del Prebético externo, evolución del estrecho orbético. Boletín Geológico y Minero de España, 5, 9-21.

Calvo, J. P., and Elízaga, E. (1994). The Cenajo and Las Minas basins (Miocene), southeastern Spain. In: Kelts Gierlowski-Kordesch (eds), Global geolog-

ical record of lake basins 1. Cambridge Univ. Press, 319-324.

Calvo, J. P., Gómez-Gras, D., Alonso-Zarza, A. M., and Jimenez, S. (2000). Architecture of a bench-type carbonate lake margin and its relation to fluvially dominated deltas, Las Minas basin, Upper Miocene, Spain. Journal of Sedimentary Research, 70, 240-254.

Calvo, J. P., Rodríguez-Pascua, M. A., and Gómez-Gras, D. (2014). Rasgos sedimentarios indicadores de inestabilidad causada por actividad tectónica sismogénica. Las cuencas neógeneas de las Minas de Hellín y Cenajo (Prebético Externo, SE de España). Revista de la Sociedad Geológica de España, 27, 205-221.

Claypool, G. E., Holser, W. T., Kaplan, I. R., Sakai, H., and Zak, I. (1980). The age curves of sulfur and oxygen isotopes in marine sulfate and their mutual interpretation. Chemical Geology, 28, 199-260.

Davis, J. B., and Kirkland, D. W. (1979). Bioepigenetic sulfur deposits. Economic Geology, 74, 462-468.

Dessau, G., Jensen, M. L., and Nakai, N. (1962). Geology and isotopic studies of Sicilian sulfur deposits. Economic Geology, 57, 410-438.

Elízaga, E. (1994). Análisis de facies sedimentarias y petrología de los depósitos lacustres de edad Neógeno Superior de la zona prebética, Albacete, España. Instituto de Estudios Albacetenses (1º etapa), 74, 216 pp.

Elízaga, E., Calvo, J. P. (1988). Evolución sedimentaria de las cuencas lacustres neógenas de la zona prebética (Albacete, España). Relación, posición y efectos del vulcanismo durante la evolución. Interés minero. Boletín Geológico y Minero de España, 69, 837-846.

Foucault, A., Calvo, J. P., Elízaga, E., Rouchy, J. M., and Servant-Vildary, S. (1987). Place des dèpots lacustres d'age miocène supérieur de la region de Hellin (Province de Albacete, Espagne) dans l'évolution géodinamique des Cordillères bétiques. Comptes Rendus de l'Académie des Sciences Paris, 305-II, 1163-1167.

Francois, R. (1986). A study of Sulphur enrichment in the humic fraction of marine sediments during early diagenesis. Geochimica et Cosmochimica Acta, 51, 17-27.

Gasiewicz, A. (2000). Comparative study of major element geochemistry of gypsum-gosht limestones and selenite lithofacies from the Miocene of northern Carpathian Foredeep: implications to the model of massive replacement of solid sulphates by calcium carbonates. Chemical Geology, 164, 183-218.

Gimeno, D. (1994). Estudio de las materias primas minerales contenidas en los materiales miocénicos lacustres de la provincia de Albacete. Revista de Estudios Albacetenses (2ª etapa), 34, 102 pp.

Hodell, D., Anselmetti, F., Brenner, M., Ariztegui, D., and PISDP Scientific Party (2006). The lake Petén Itzá, Scientific Drilling Project. Scientific Drilling, 3, 25-29.

Ivanov, M. V. (1968). Microbial processes in the formation of sulfur deposits. Israel Program for Scientific Translations, IPST Cat. Nº 1850, U.S: Dept. Commerce, 298pp. (English translation from Russian).

Jassin, S. Z., Raiswell, R., and Botrell, S. H. (1999). Genesis of the Middle Miocene stratabound sulphur of Northern Iraq. Journal of Geological Society, London, 156, 25-39.

Jørgensen, B. B. (1977). The sulfur cycle of a coastal marine sediment (Limfjorden, Denmarck). Limnology and Oceanography, 22, 814-832.

Kaplan, I. R., Emery, K. O., and Rittenberg, S. C. (1963). The distribution and isotopic abundance of sulphur in recent marine sediments of southern California. Geochimica et Cosmochimica Acta, 27, 297-331.

Labrado, A. L., Brunner, B., Bernasconi, S. M., and Peckmann, J. (2019). Formation of large native sulfur deposits does not require molecular oxygen. Frontiers in Microbiology, 10. https://doi.org/10.3389/fmicb.2019.00024.

Lewin, J. C. (1961). The dissolution of silica from diatom walls. Geochimica et Cosmochimica Acta, 21, 182-198.

Lindtke, J., Ziegenbalg, S. B., Brunner, B., Rouchy, J. M., Pierre C., and Peckmann, J. (2011). Authigenesis of native sulphur and dolomite in a lacustrine evaporitic setting (Hellín basin, Late Miocene, SE Spain). Geological Magazine, 148, 655-669.

Machel, H. G. (2001). Bacterial and thermochemical sulfate reduction in diagenetic settings – old and new insights. Sedimentary Geology, 140, 143-175.

Margalef, R. (1955). Observaciones paleoecológicas y geocronológicas sobre los sedimentos lacustres miocénicos de Hellín (Albacete). Memorias y comunicaciones, Instituto Geológico de Barcelona, 10, 53-72.

Martín, J. M., Puga-Bernabéu, A., Aguirre J., and Braga, C. (2014). Miocene Atlantic-Mediterranean seaways in the Betic Cordillera (Southern Spain). Revista de la Sociedad Geológica de España, 27, 175-186.

Martín-Velázquez, S., de Vicente, G., Rodríguez-Pascua, M. A., and Calvo, J. P. (1998). Análisis dinámico del sistema de desgarres NO-SE del Prebético de Albacete. Revista de la Sociedad Geológica de España, 11, 369-383.

Meseguer, J. (1924). Estudio de los yacimientos de azufre de las provinicias de Murcia y Albacete. Boletín del Instituto Geológico y Minero de España, 45, 133-214.

Nobel, F. A., Ansriessen, P. A. M., Hebeda, P. H., Priem, H. N. A., and Rondeel, E. H. (1981). Isotopic datting of the postalpine Neogene volcanism in

the Betic cordilleras, Southern Spain. Geologie en Mijnbouw, 60, 209-214.

Nrigu, J. O. (1968). Sulfur metabolism and sedimentary environment: Lake Mendota, Wisconsin. Limnology and Oceanography, 13, 430-439.

Ortí, F., Rosell, L., and Anadón, P. (2010). Diagenetic gypsum related to sulfur deposits in evaporites (Libros Gypsum, Miocene, NE Spain). Sedimentary Geology, 228, 304-318.

Ortí, F., Pérez-López, A., García-Veigas, J., Rosell, L., Cendón, D. I., Pérez-Valera, F. (2014a). Sulfate isotope compositions ($\delta^{34}S$, $\delta^{18}O$) and strontium isotopic ratios ($^{87}Sr/^{86}Sr$) of Triassic evaporites in the Betic Cordillera (SE Spain). Revista de la Sociedad Geológica de España, 27, 79-89.

Ortí, F., Rosell, L., Gibert, L., Moragas, M., Playà, E., Ingles, M., Rouchy, J. M., Calvo, J. P., and Gimeno, D. (2014b). Evaporite sedimentation in a tectonic active basin: The lacustrine Las Minas Gypsum unit (Late Tortonian, SE Spain). Sedimentary Geology, 311, 17-42.

Parafiniuk, J. (1989). Oxidation of native sulfur in the Fore-Carpathian sulfur deposits in the light of isotopic and mineralogical data. Acta Geologica Polonica, 39, 113-122.

Passier, H., Middelburg, J. J., De Lange, G. J., and Böttcher, M. E. (1999). Modes of sapropel formation in the eastern Mediterranean: some constraints based on pyrite properties. Marine Geology, 153, 199-219.

Pawlowski, S., Pawlowska, K., and Kubica, B. (1979). Geology and genesis of Polish sulfur deposits. Economic Geology, 74, 475-483.

Paytan, A., Kastner, M., Campbell, D., and Thiemens, M. H. (1998). Sulfur isotopic composition of Cenozoic seawater sulfate. Science, 282, 1459-1462.

Peckmann, J., Paul, J., and Thiel, V. (1999). Bacterially mediated formation of diagenetic aragonite and native sulfur in Zechstein carbonates (Upper Permian, Central Germany). Sedimentary Geology, 126, 205-222.

Permanyer, A., Jorge, R. Baudino, R., and Gibert, L. (2016). Organic-rich shales from internal Betic basins (SE Spain): potential source rocks for the pre-Messinian Salt play in the western Mediterranean. Geologica Acta, 14, 443-460.

Phillip, G., Wali, A. M. A., and Aref, M. A. M. (1994). On the origin of native sulfur deposits in Gebel el Zeit, Gulf of Suez, Egypt. Carbonates and Evaporites, 9, 223-232.

Pierre, C., and Rouchy, J. M. (1988). Carbonate replacements after sulfate evaporites in the middle Miocene of Egypt. Journal of Sedimentary Petrology, 58, 446-456.

Pineda, V., Gibert, L., Soria, J. M., Carrazana, A., Ibáñez-Insa, J., and Sánchez-Román, M. (2021). Interevaporitic deposits of Las Minas Gypsum Unit: a record of Late Tortonian marine incursions and dolomite precipitation in Las Minas Basin (eastern Betic Cordillera, SE Spain). Paleogeography, Palaeoclimatology, Palaeoecology, 564, 110171.

Playà. E., Ortí, F., and Rosell, L. (2000). Marine to non-marine sedimentation in the upper Miocene evaporites of the Eastern Betics, SE Spain: sedimentological and geochemical evidence. Sedimentary Geology, 133, 135-166.

Pozo, M., Calvo, J. P., Scopelliti, G., and González-Acebrón, L. (2016). Seepage carbonate mounds in Cenozoic sedimentary sequences from the Las Minas Basin, SE Spain. Sedimentary Geology, 334, 1-20.

Rodríguez-Pascua, M. A., de Vicente, G., and Calvo, J. P. (2001). Paleoseismological analysis of late Miocene lacustrine sediments in the Prebetic Zone, SE Spain. Acta Geológica Hispánica, 36, 213-232.

Rodríguez-Pascua, M. A., de Vicente, G., Calvo, J. P., and Pérez-López, R. (2003). Similarities between recent seismic activity and paleoseismites during the late Miocene in the external Betic Chain (Spain): relationship by 'b' value and the fractal dimension. Journal of Structural Geology, 25, 749-763.

Rouchy, J. M., Taberner, C., Blanc-Valleron, M. M., Sprovieri, R., Rusell, M., Pierre, C., Di Stefano, E., Pueyo, J. J., Caruso, A., Dinares-Turell, E., Gomis-Coll, E., Wolff, G. A., Cespuglio, G., Ditchfield, P., Pestrea, S., Combourieu-Nebout, N., Santisteban, C., and Grimalt, J. O. (1998). Sedimentary and diagenetic markers of the restriction in a marine basin: the Lorca Basin (SE Spain) during the Messinian. Sedimentary Geology, 121, 23-55.

Ruckmick, J. C., Wimberly, B. H., and Edwards, A. F. (1979). Classification and genesis of biogenic sulfur deposits. Economic Geology, 74, 469-474.

Sánchez-Román, M., McKenzie, J. A., Rebello Wagener, A., Rivadeneyra, M. A., and Vasconcelos, C. (2009). Presence of sulfate does not inhibit low-temperature dolomite precipitation. Earth and Planetary Science Letters, 285, 131-139.

Sánchez-Román, M., Romanek, Ch. S., Fernández-Remolar, D. C., Sánchez-Navas, A., McKenzie, J. A., Amils Pibernat, R., and Vasconcelos, C. (2011). Aerobic biomineralization of Mg-rich carbonates: implications for natural environments. Chemical Geology, 281, 143-150.

Sanz de Galdeano, C., and Vera, J. A. (1992). Stratigraphic record and palaeogeographical context of the Neogene basins in the Betic Cordillera, Spain. Basin Research, 4, 21-36.

Servant-Vildary, S., Rouchy, J. M., Pierre, C., and Foucault, A. (1990). Marine and continental water contributions to a hypersaline basin using diatom ecology, sedimentology, and stable isotopes: an example in the Late Miocene of Mediterranean (Hellín basin, southern Spain). Palaeogeography, Palaeoclimatology, Palaeocology, 79, 189-204.

Tekin, E. (2006). Elemental sulfur of bacterial origin in the lacustrine evaporites of the Polatli-Sivrihisar Neogene basin (Central Anatolia, Turkey). Carbonates and Evaporites, 21, 33-39.

Troelsen, H., and Jørgensen, B. B. (1981). Seasonal dynamics of elemental sulfur in two coastal sediments. Estuarine, Coastal and Shelf Science, 15, 255-266.

van Lith Y., Vasconcelos, C., Warthmann, R., Martins, J., and McKenzie, J. (2002). Bacterial sulfate reduction and salinity: two controls on dolomite precipitation in Lagoa Vermelha and Brejo do Espinho (Brazil). Hydrobiologia, 485, 35-49.

Vasconcelos, C., and McKenzie, J. A. (1997). Microbial mediation of modern dolomite precipitation and diagenesis under anoxic conditions (Lagoa Vermelha, Rio de Janeiro, Brazil). Journal Sedimentary Research, 67, 378-390.

Warthmann, R., van Lith, Y., Vasconcelos, C., McKenzie, J. A., and Karpoff, A. M. (2000). Bacterially induced dolomite precipitation in anoxic culture experiments. Geology, 28, 1091-1094.

Wijsman, J. W. N., Middelburg, J. J., Herman, P. M. J., Böttcher, M., and Heip, C. H. R. (2001). Sulfur and iron speciation in surface sediments along the northwestern margin of the Black Sea. Marine Chemistry, 74, 261-278.

Ziegenbalg, S. B., Brunner, B., Rouchy, J. M., Birgel, D., Pierre, C., Böttcher, M. E., Caruso, A., Immenhauser, A., and Peckmann, J. (2010). Formation of secondary carbonates and native sulphur in sulphate-rich Messinian strata, Sicily. Sedimentary Geology, 227, 37-50.